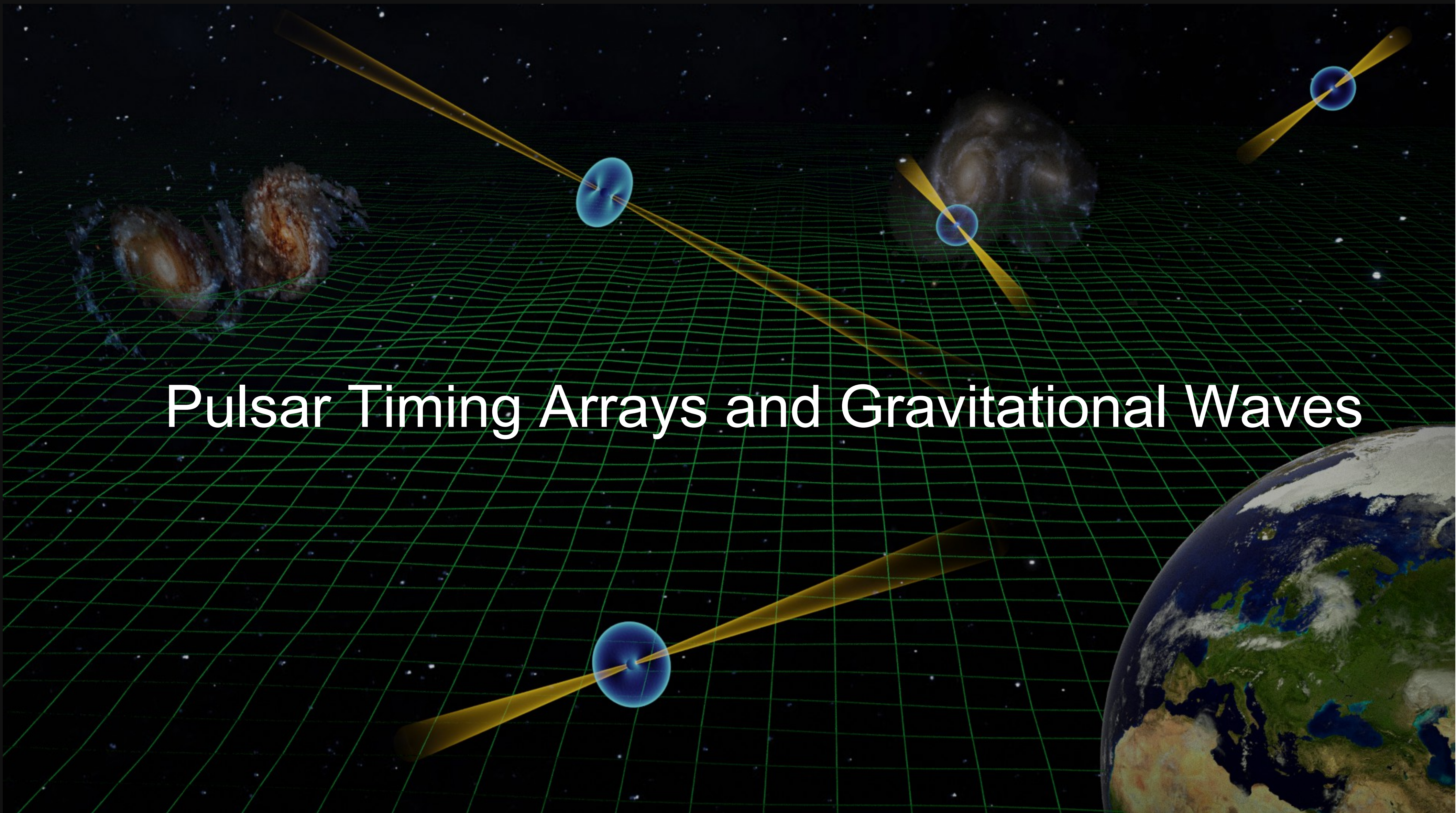

Pulsar Timing Arrays and Gravitational Waves

Gilles Theureau,
LPC2E/CNRS and Observatoire de Paris

Context

NANOGrav : Arzoumanian et al, December 2020
PPTA : Goncharov et al, August 2021
EPTA : Chen et al, December 2021
IPTA : Antoniadis et al, March 2022

« On the Evidence for a Common-spectrum Process in the Search for the nHz Gravitational-wave Background »

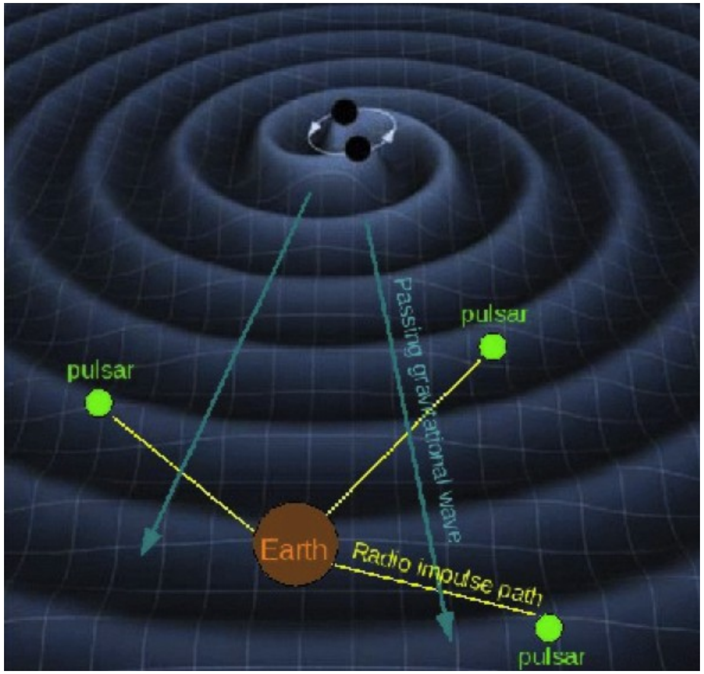

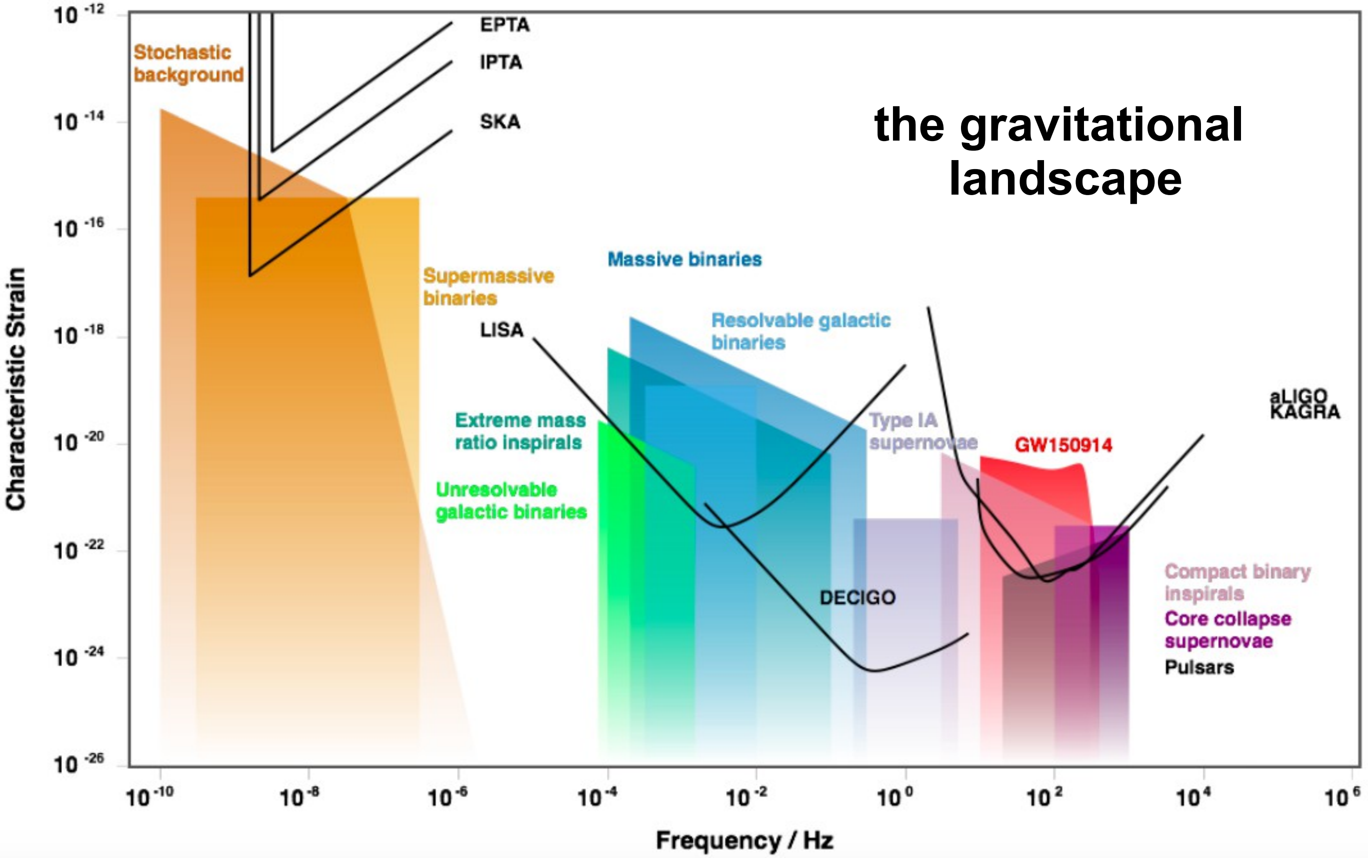

the gravitational landscape

The nanoHertz domain

- **Super Massive Black Hole Binaries (SMBHB)**

- **Cosmic string loops**

- **Relics of inflation** (e.g. quantum fluctuations of the gravitational field in the early universe, amplified by an inflationary phase

- **First-order phase transition** (e.g. due to MHD turbulence induced by primordial magn field)

Pulsars = fastly rotating neutron stars

Supernova explosion of a massive star (**> 9 M_{sun}**)

Core collapse in a neutron star of **1.3-2.2 M_{sun}**

Huge magnetic field: **10^{8} - 10^{14} Gauss**

Rotation periods: **0.001-10 seconds**

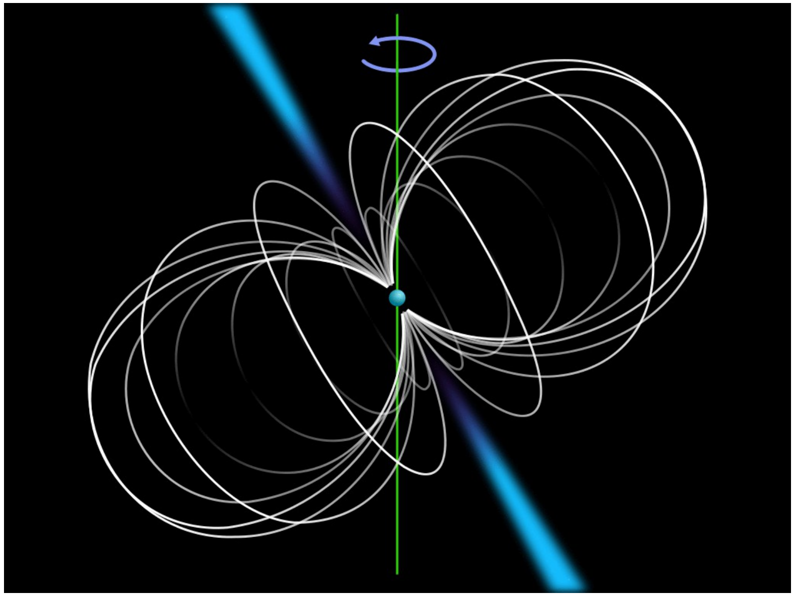

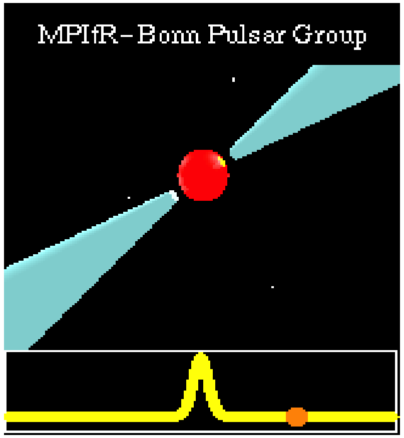

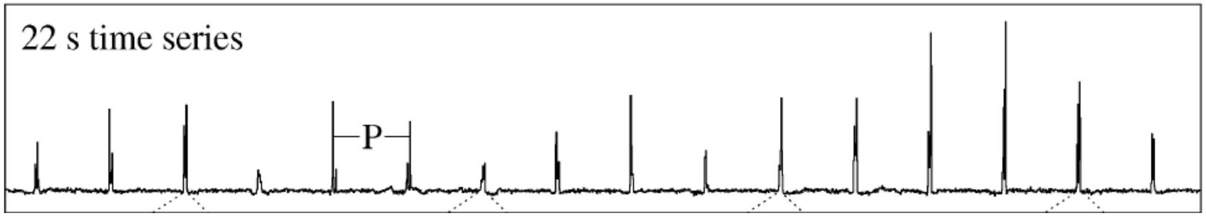

Pulsars = fastly rotating neutron stars

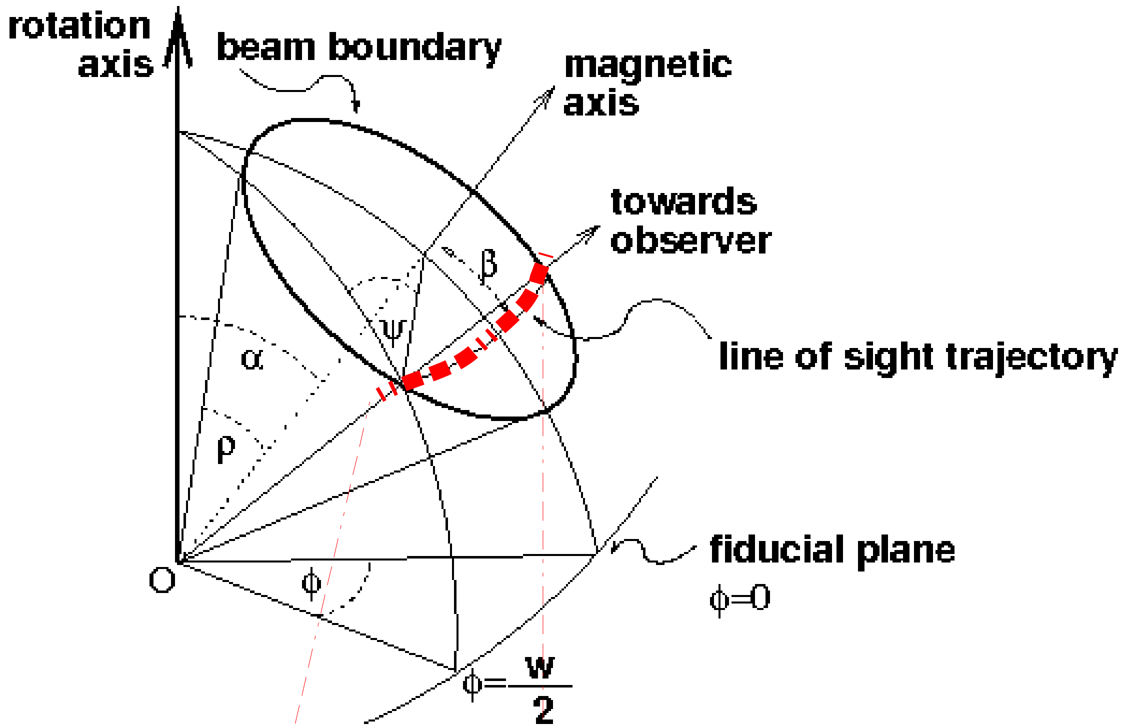

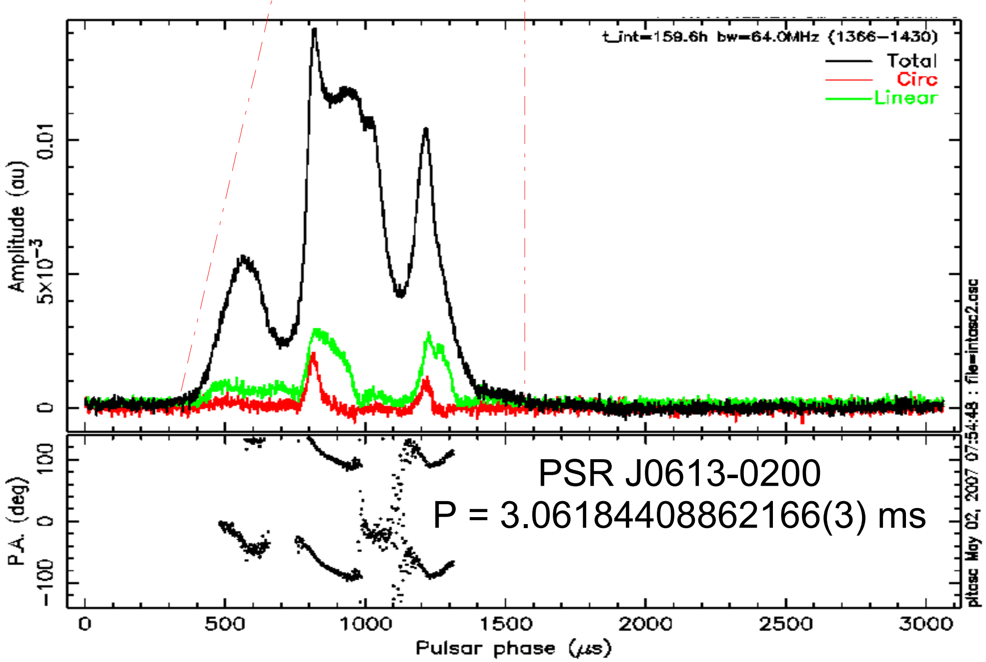

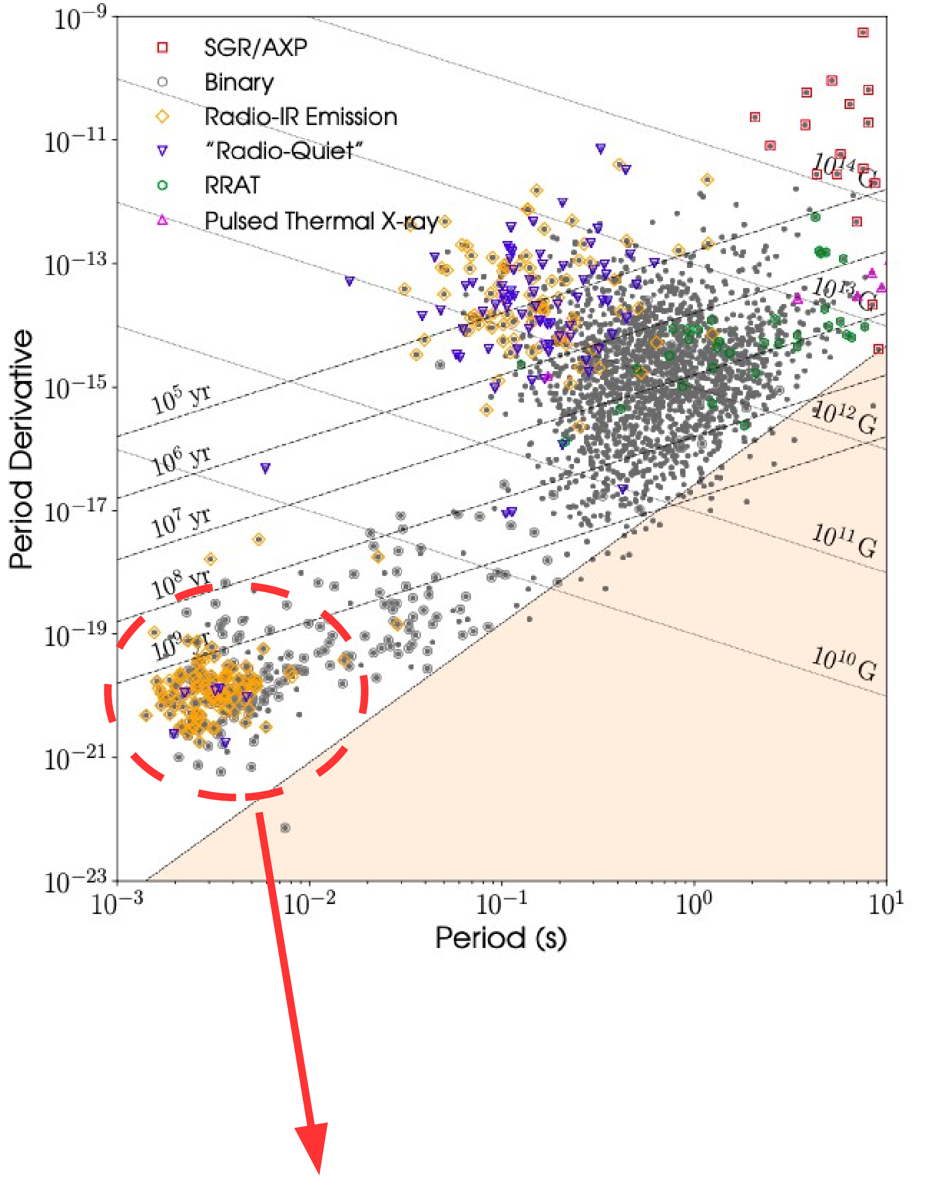

Millisecond pulsar population

very stable rotation < 1μs rms over years

The art of timing

I – the de-dispersion problem

The lowest frequencies are delayed

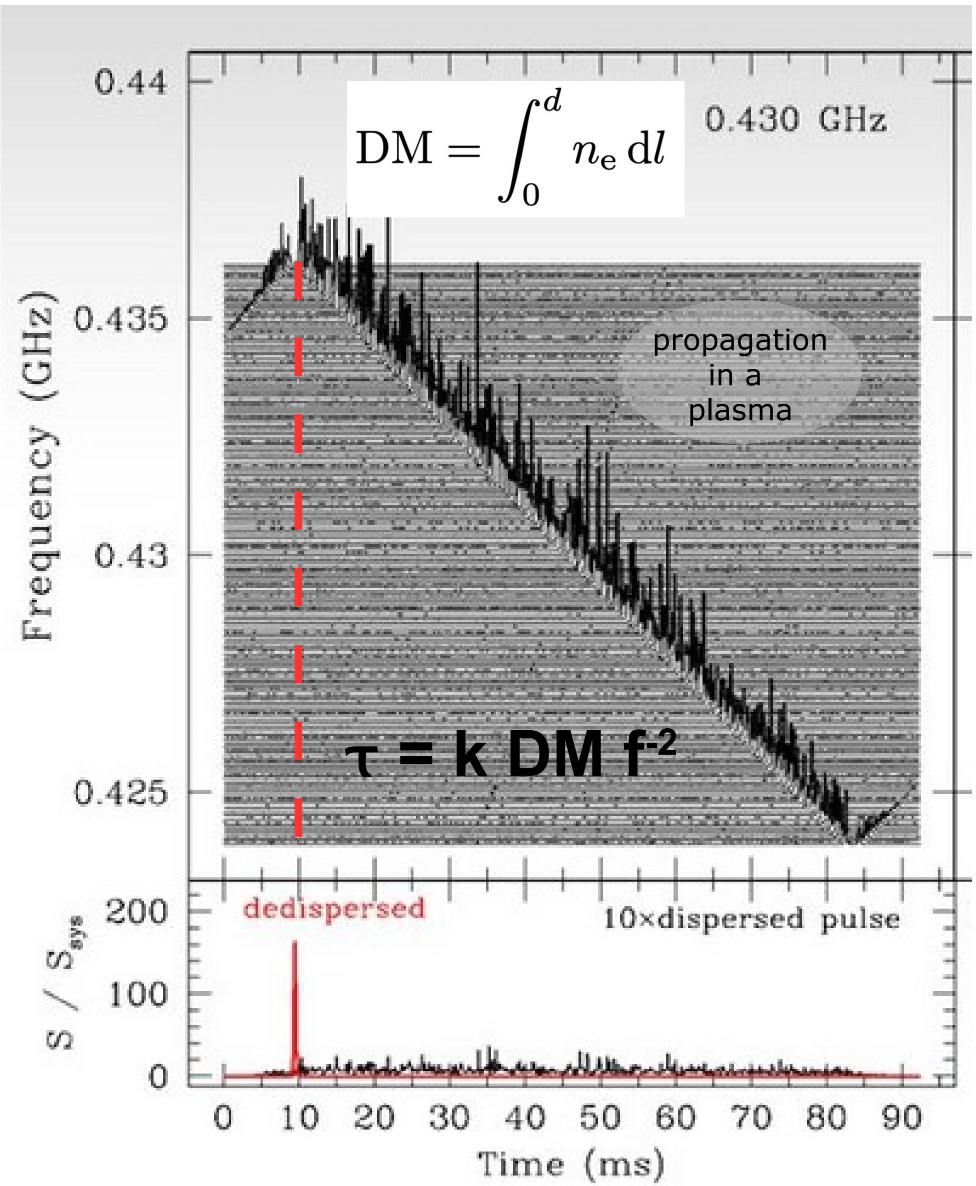

II- phase folding with rotation

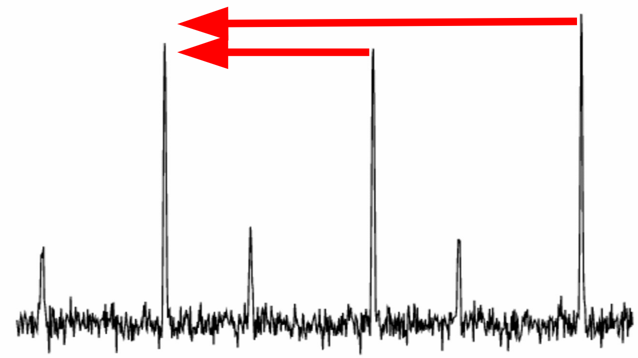

According to a model :
slow down,
orbital motion,
proper motion
planetary ephem.

III – Time stamping

(Time of arrival computation)

« TOA »

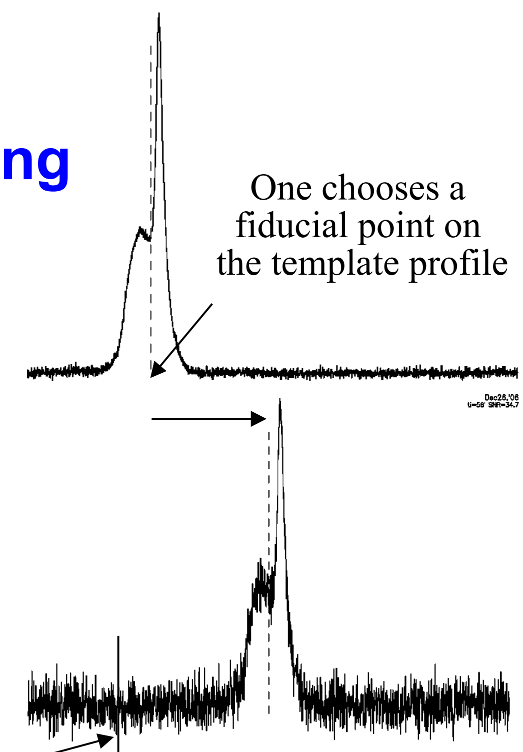

Position of the first data sample, corresponding to start of observation

The art of timing

I – the de-dispersion problem

The lowest frequencies are delayed

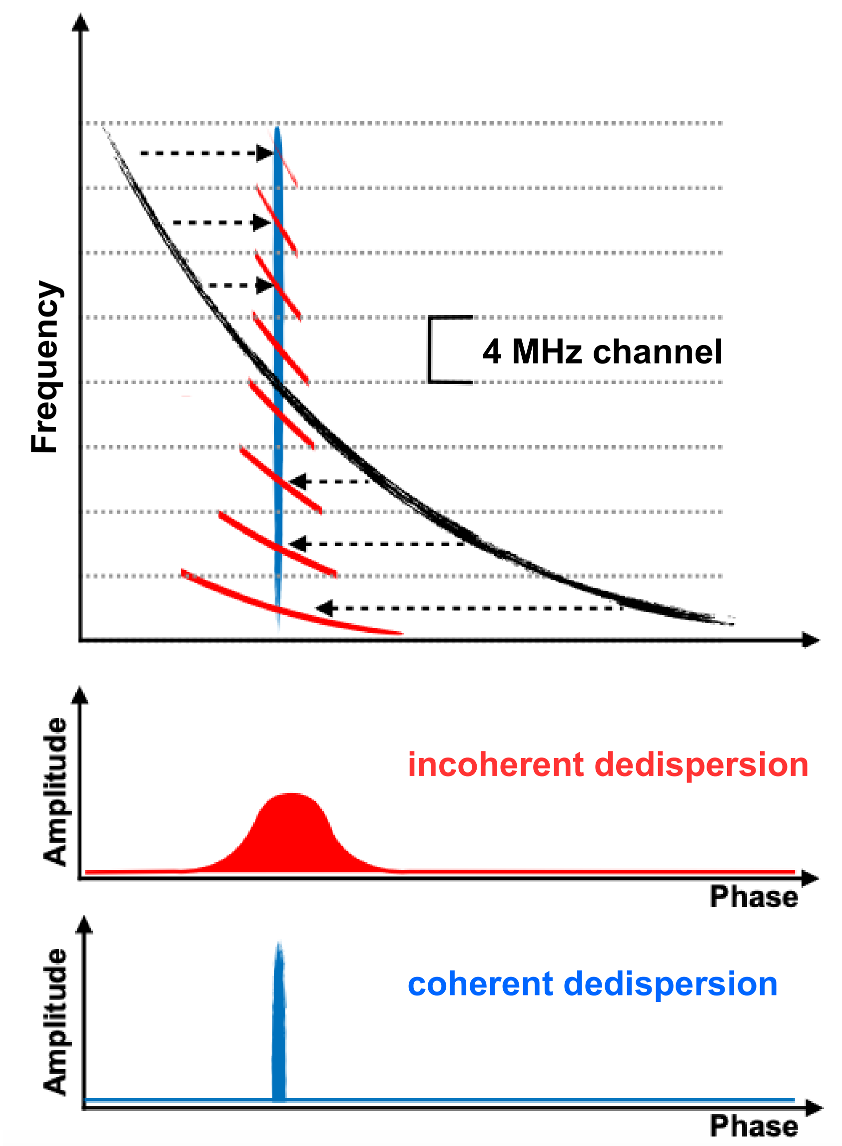

II- phase folding with rotation

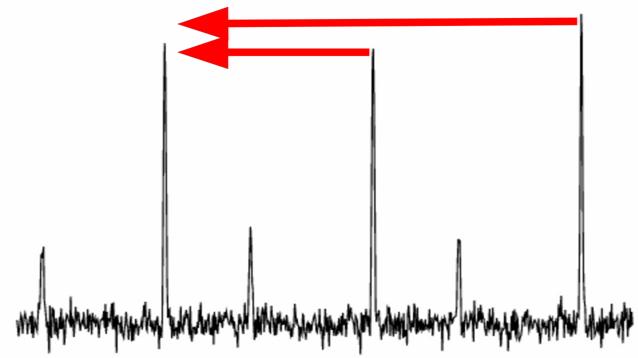

According to a model :
slow down,
orbital motion,
proper motion
planetary ephem.

III – Time stamping

(Time of arrival computation)

« TOA »

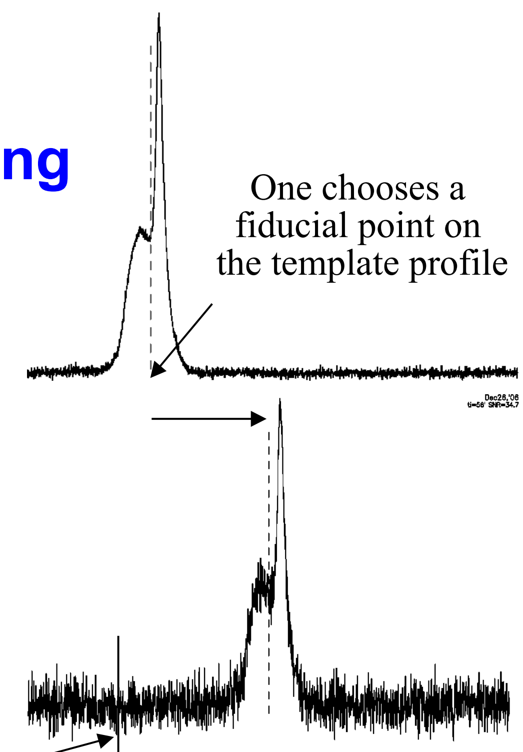

One chooses a fiducial point on the template profile

Position of the first data sample, corresponding to start of observation

Looking for extreme timing precision

the timing uncertainty can go down to 10-20 ns for some pulsars.

$$\sigma_{\mathrm{TOA}} \propto \frac{w}{S_{\mathrm{PSR}}} \frac{T_{\mathrm{sys}}}{A} \frac{1}{\sqrt{BT}}$$

Weak fluxes ~mJy (1 Jy = 10^{-26} W/m^2)

→ **requires wide band pass in frequency**

→ **requires a large radio telescope**

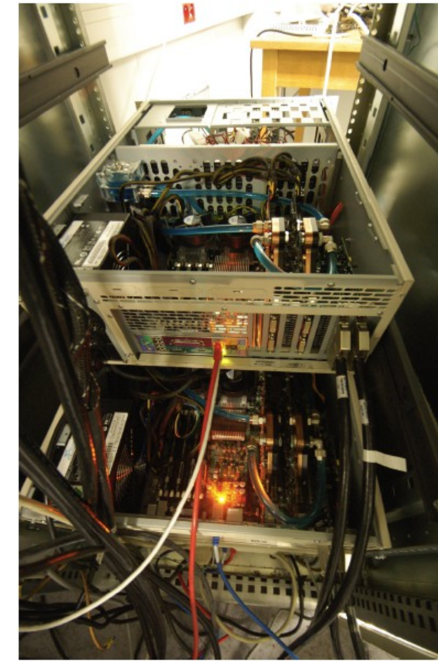

Current instrumentation in Nançay:
Coherent dedispersion over 512 MHz
4 PCs / 8 GPUs (16 Gb / s flux)

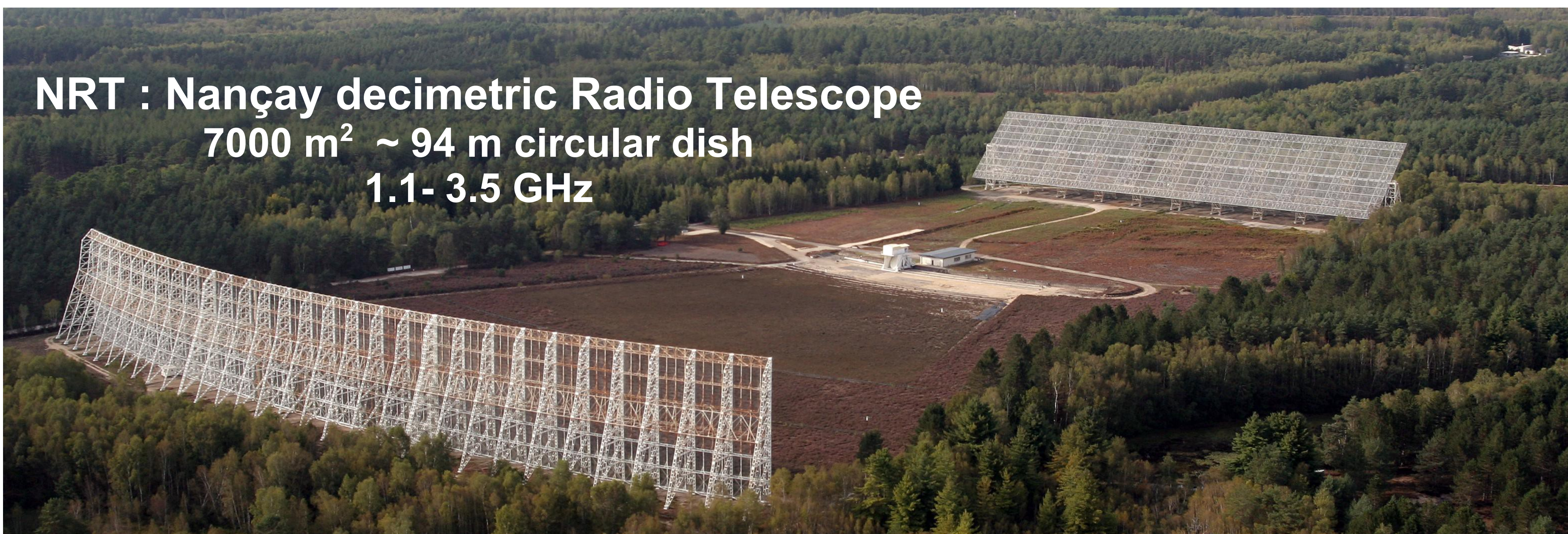

The International Pulsar Timing Array

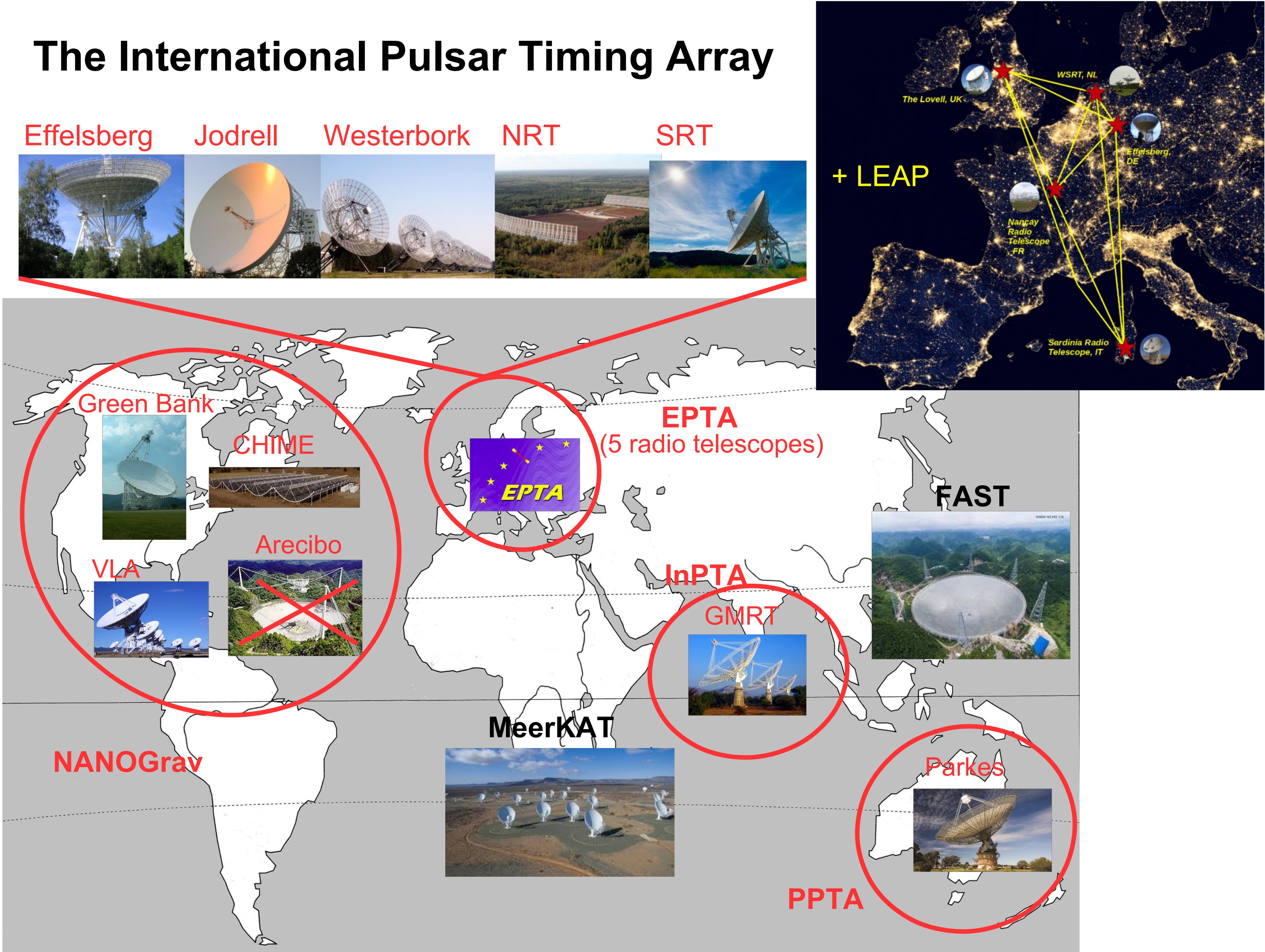

Pulsar Timing Arrays : principles

The Earth and the distant pulsar are considered as free masses whose position responds to changes in the metric of space-time

→ *The passage of a gravitational wave disturbs the metric and produces fluctuations in the arrival times of the pulses*

With timing uncertainties dt (~100 ns) and observation time spans T (~25 years)
→ PTA are sensitive to *amplitudes ~ dt/T and to frequencies f ~ 1/T*

Sensitivity ~ 100 10^{-9} / 25 x 3 10^{7} → **A ~ 1.3 10^{-16}**

Frequency domain (25 years - 1 week) → **10^{-9} – 10^{-6} Hz**

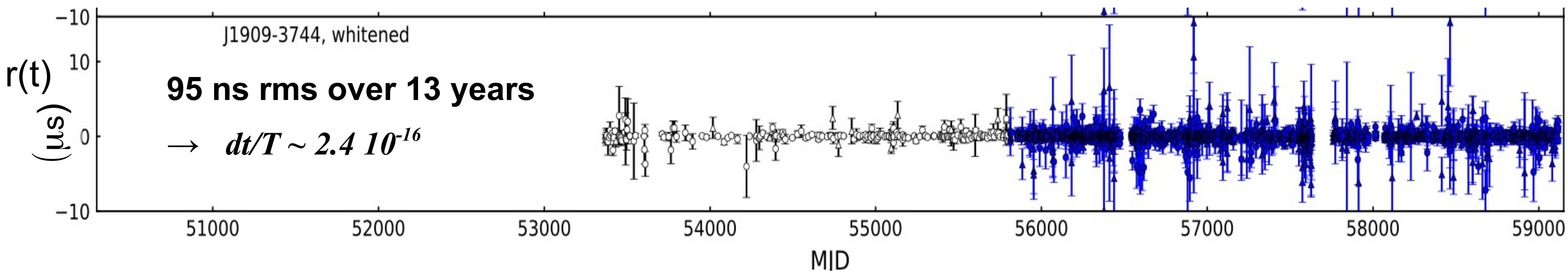

Pulsar Timing Arrays : principles

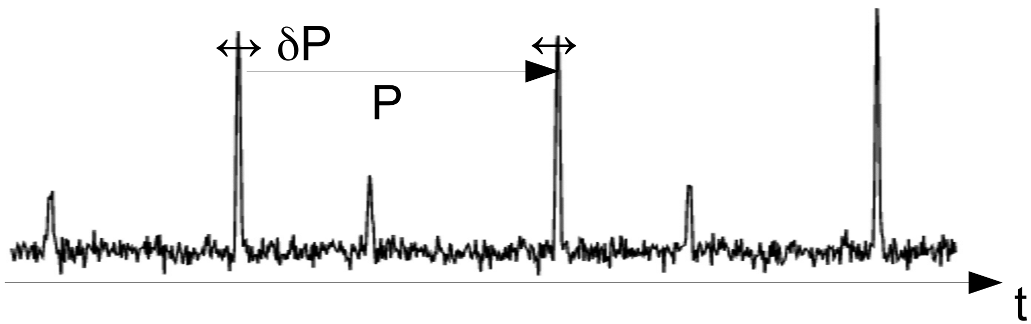

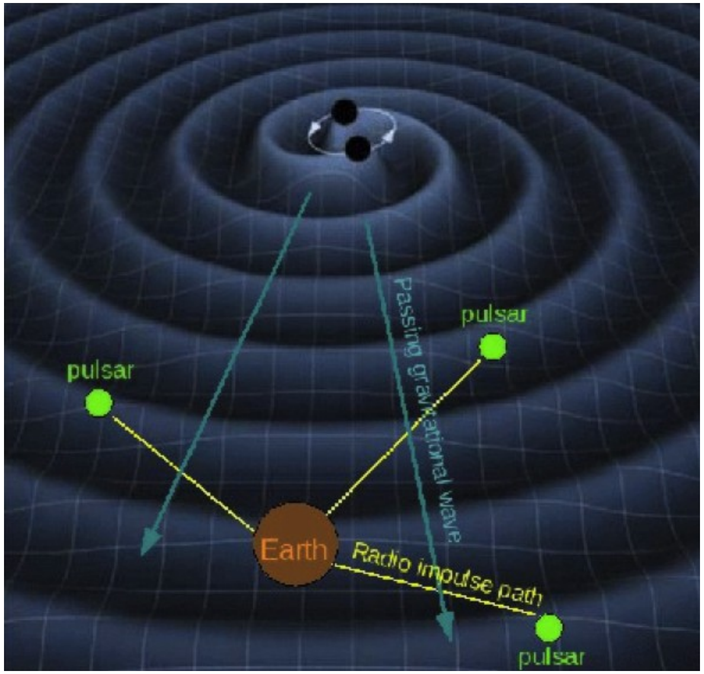

Analysis of time residuals

$$r(t) = \int_0^t \frac{\delta\nu}{\nu}(t')dt'$$

$$\frac{\delta\nu}{\nu}(t) = \frac{1}{2}\frac{\hat{n}^i\hat{n}^j}{1+\hat{n}.\hat{k}}(h_{ij}(t - L(1+\hat{k}.\hat{n})) - h_{ij}(t))$$

pulsar-Earth distance

dir pulsar

dir GW source

wave amplitude at the pulsar

wave amplitude at the Earth

Pulsar Timing Arrays : principles

1) Describe the pulsar rotation in a reference frame co- moving with the pulsar

$$\nu(t) = \nu_0 + \dot{\nu}_0(t - t_0) + \frac{1}{2}\ddot{\nu}_0(t - t_0)^2 + \cdots$$

The observed parameters ν and ν are associated with the physical processes causing pulsars to spin down

2) Timing model

$$t_{SSB} = t_{topo} + \overbrace{t_{corr} - \delta D/f_{obs}^2 + \Delta_{R\odot} + \Delta_{\pi} + \Delta_{S\odot} + \Delta_{E\odot} + \Delta_R + \Delta_S + \Delta_E + \Delta_A}^{\boldsymbol{\tau}^{\mathrm{TM}}}$$

clock

dispersion

Solar System
Römer, parallax, Shapiro
and Einstein delays

binary system
Römer, Shapiro, Einstein
and Aberration delays

Pulsar Timing Arrays : principles

2) Timing model (examples)

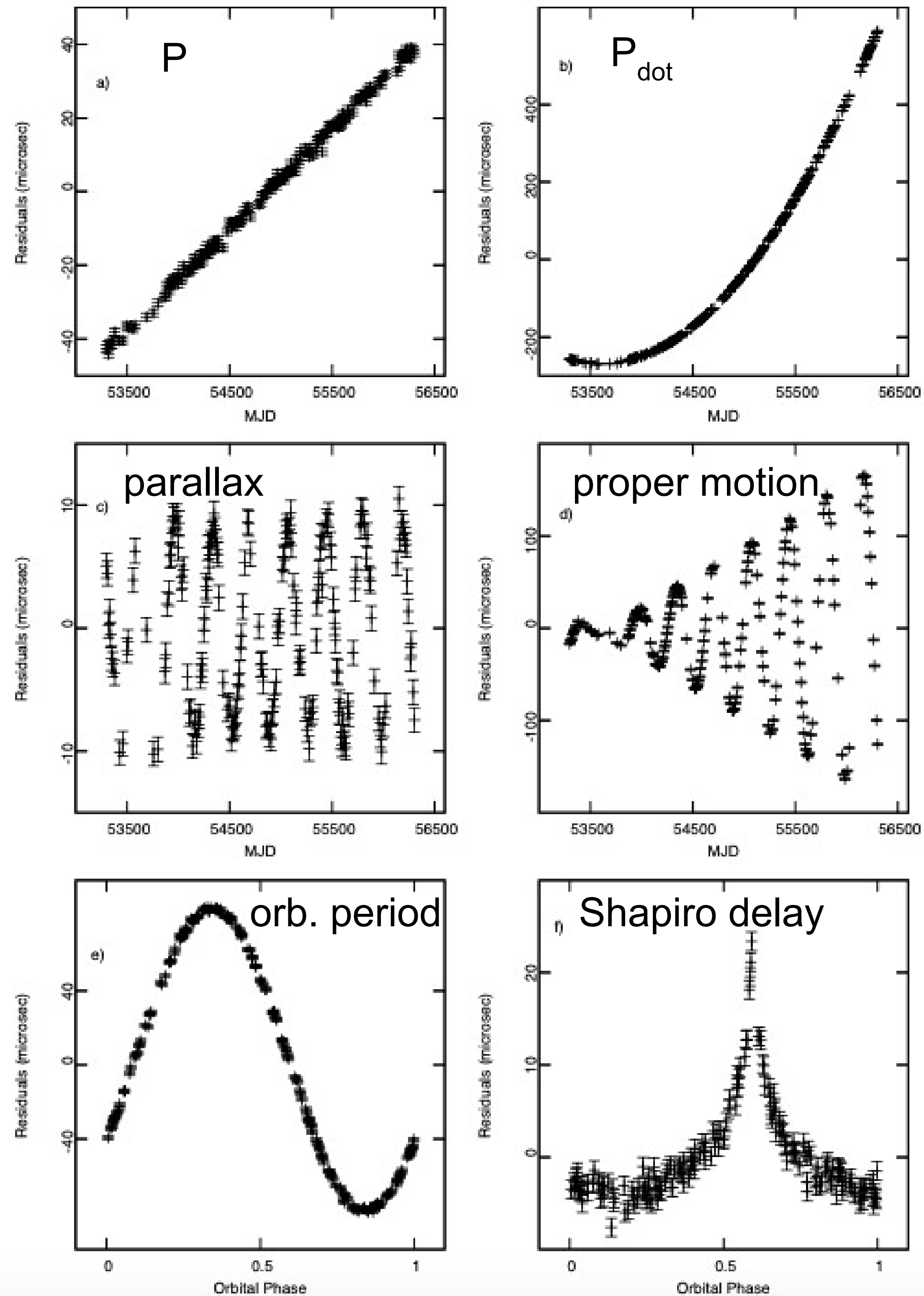

Pulsar Timing Arrays : principles

1) Describe the pulsar rotation in a reference frame co- moving with the pulsar

$$\nu(t) = \nu_0 + \dot{\nu}_0(t - t_0) + \frac{1}{2}\ddot{\nu}_0(t - t_0)^2 + \cdots$$

The observed parameters ν and ν are associated
with the physical processes causing pulsars to spin down

2) Timing model

$$t_{SSB} = t_{topo} + \overbrace{t_{corr} - \delta D/f_{obs}^2 + \Delta_{R\odot} + \Delta_{\pi} + \Delta_{S\odot} + \Delta_{E\odot} + \Delta_{R} + \Delta_{S} + \Delta_{E} + \Delta_{A}}^{\boldsymbol{\tau}^{\mathrm{TM}}}$$

- t_{corr}: clock
- $\delta D/f_{obs}^2$: dispersion
- $\Delta_{R\odot} + \Delta_{\pi} + \Delta_{S\odot} + \Delta_{E\odot}$: Solar System Römer, parallax, Shapiro and Einstein delays
- $\Delta_{R} + \Delta_{S} + \Delta_{E} + \Delta_{A}$: binary system Römer, Shapiro, Einstein and Aberration delays

3) Full noise model

$$\text{observed TOA} = \boldsymbol{\tau}^{\mathrm{TM}} + \overbrace{\boldsymbol{\tau}^{\mathrm{WN}} + \boldsymbol{\tau}^{\mathrm{SN}} + \boldsymbol{\tau}^{\mathrm{DM}} + \boldsymbol{\tau}^{\mathrm{CN}}}^{\text{Noise model}} + \boldsymbol{\tau}^{\mathrm{GW}}$$

- $\boldsymbol{\tau}^{\mathrm{TM}}$: Timing Model (deterministic)
- $\boldsymbol{\tau}^{\mathrm{WN}}$: meas. (white) noise
- $\boldsymbol{\tau}^{\mathrm{SN}}$: pulsar spin (red) noise
- $\boldsymbol{\tau}^{\mathrm{DM}}$: DM (red) noise
- $\boldsymbol{\tau}^{\mathrm{CN}}$: Clock Ephem. Astroph. (red) noise
- $\boldsymbol{\tau}^{\mathrm{GW}}$: GWB (red) noise

Pulsar Timing Arrays : principles

Example : PSR J1909-3744

including timing model

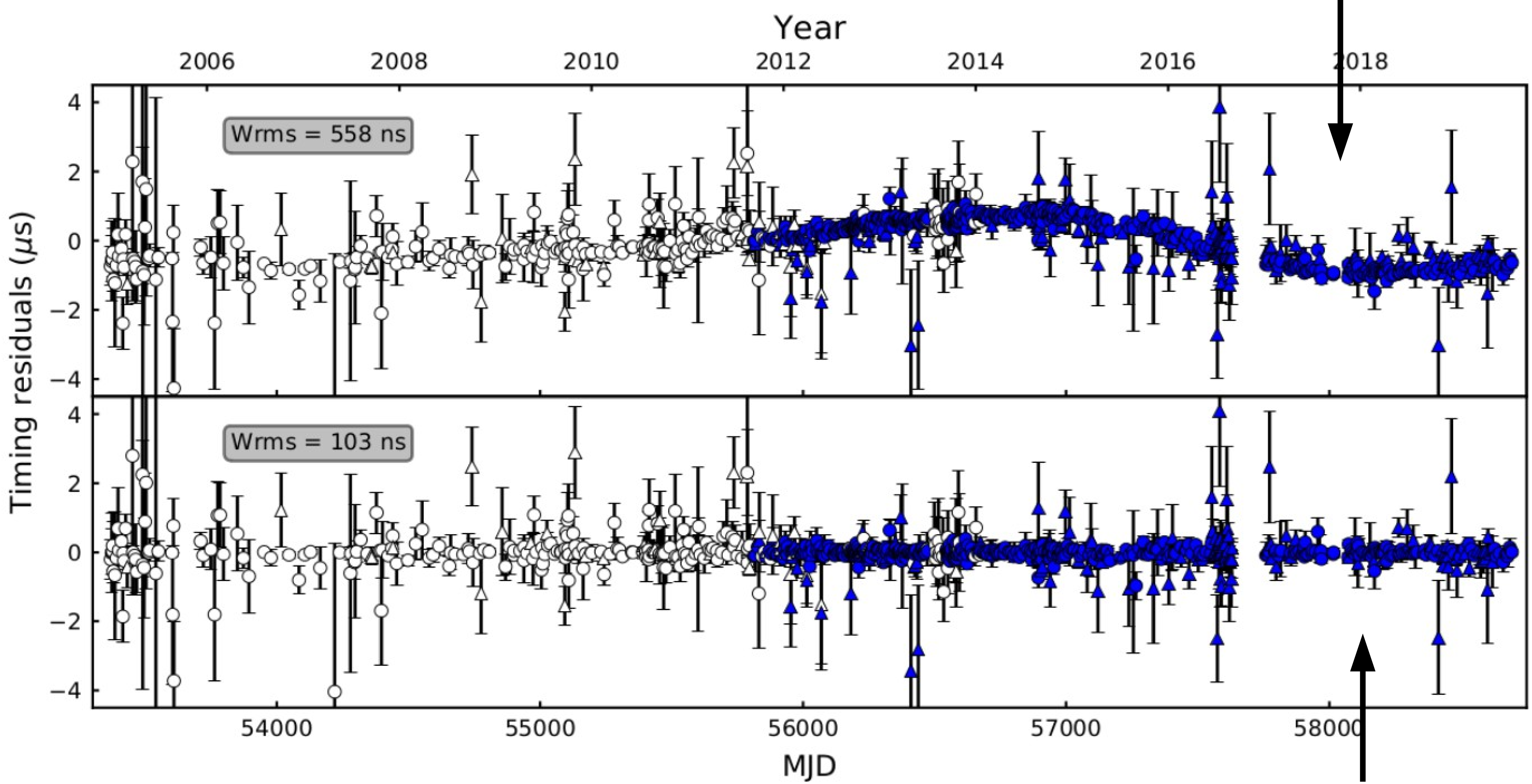

including timing model + noise model

Analysis of foregrounds: characterisation and separation of the noise components

« White noises » (un-correlated noise) $\hat{\sigma}^2 = (\sigma \cdot \mathrm{EFAC})^2 + \mathrm{EQUAD}^2$

τ^{WN}

Instrumental → telescope gain stability, pass band, backend used

Astrophysical → 'pulse jitter' (statistics of variations in pulsar magnetosphere)

« Red noises » (correlated noise) $S \propto A^2 f^{-\gamma}$

τ^{DM} Variations in the Dispersion Measure → changes « e- » content along line of sight (chromatic : multi-frequency measurements)

τ^{SN} Intrinsic rotation noise → perturbation from small bodies disc ? variations in radiated energy ? series of micro-glitches ?

τ^{CN}

Clock variations → clock-telescope link → TAI → TT-BIPM

Solar System ephemerides → position of SS barycentre → links to INPOP, JPL

Galactic motion of the Sun → LSR

τ^{GW} Gravitational waves → indiv. sources, stochastic background, « bursts » events

Pulsar Timing Arrays : principles

Pulse jitter

PSR B1919+21
P = 1.3 s

Pulsar Timing Arrays : principles

Pulse jitter

PSRJ1713+0747
P = 4.57 ms
LEAP Observations
'pulse to pulse' variations
(Bassa et al 2015)
1% in phase ↔ ~100 ns over 1 h

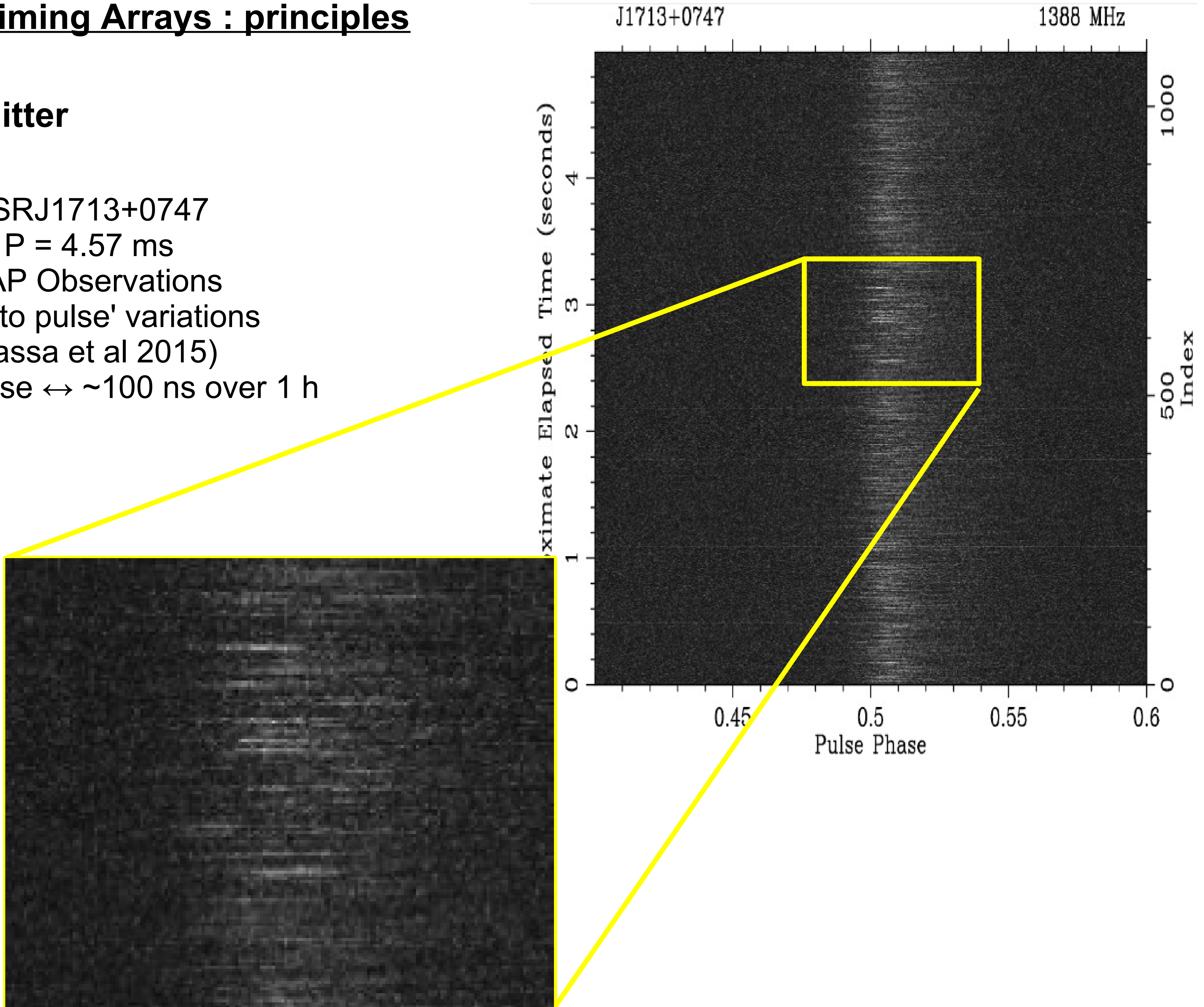

Red noise : dispersion noise or chromatic noise

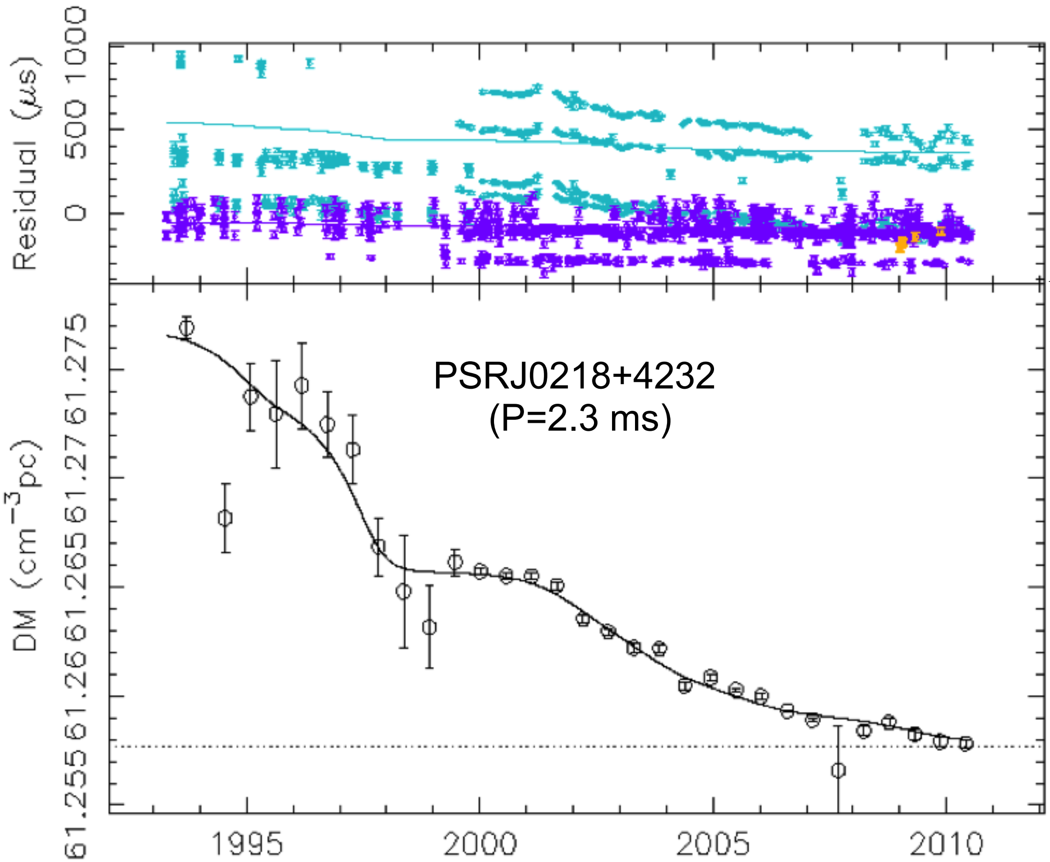

Janssen 2015

= effects of interstellar medium

Secular variation of the Dispersion Measure (due to relative proper motion)

DM events: lense effect due to a plasma bubble along the line of sight

INTERSTELLAR MEDIUM EVENTS IN PSR J1713+0747

Lam et al 2018

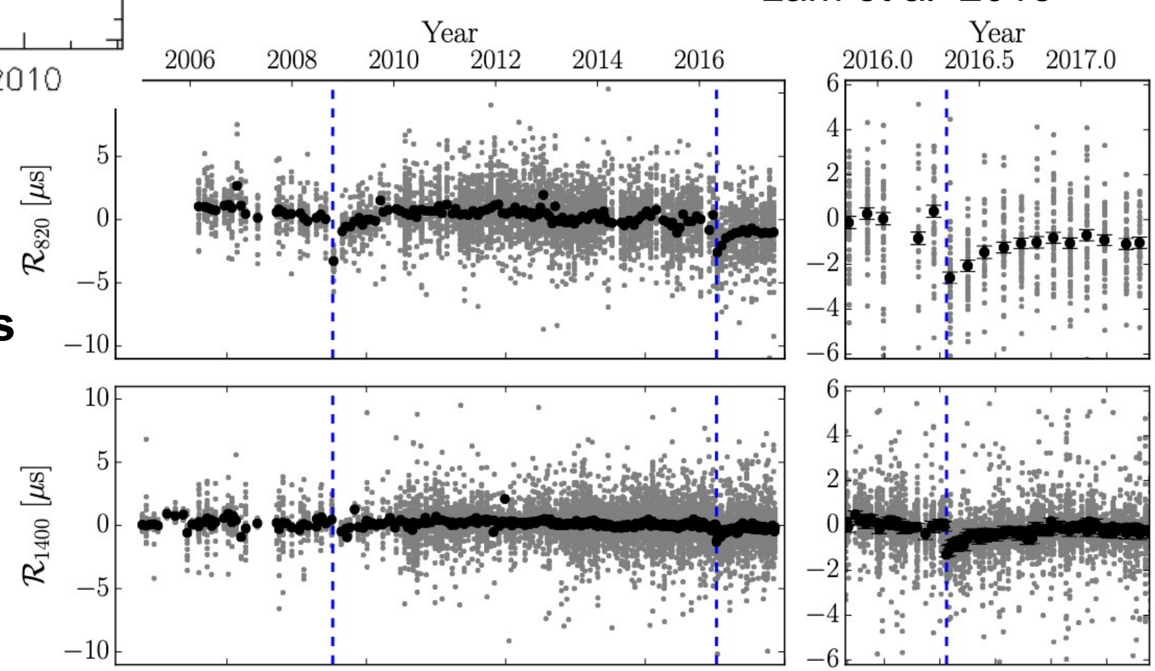

requires multi-wavelength observations e.g. 500 MHz, 1400 MHz, 2.5 GHz

Red noise : spin noise

P=1.55 ms rms ~ 34 .5 μs <unc.> ~ 60 ns

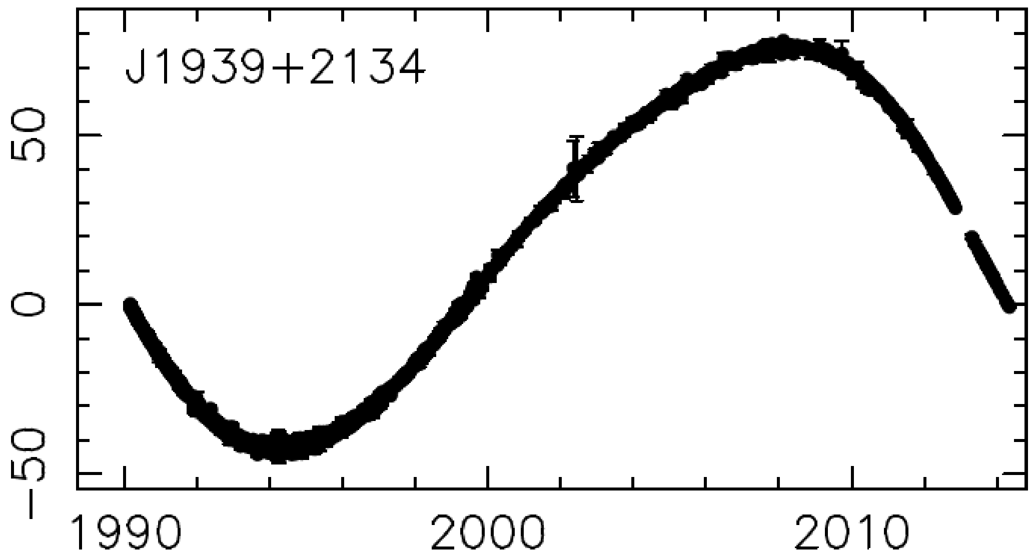

P=2.9 ms rms ~ 0.092 μs <INC‰> ~ 60 ns

Small bodies disc perturbation ?

E_{dot} variations?

Series of micro-glitches ?

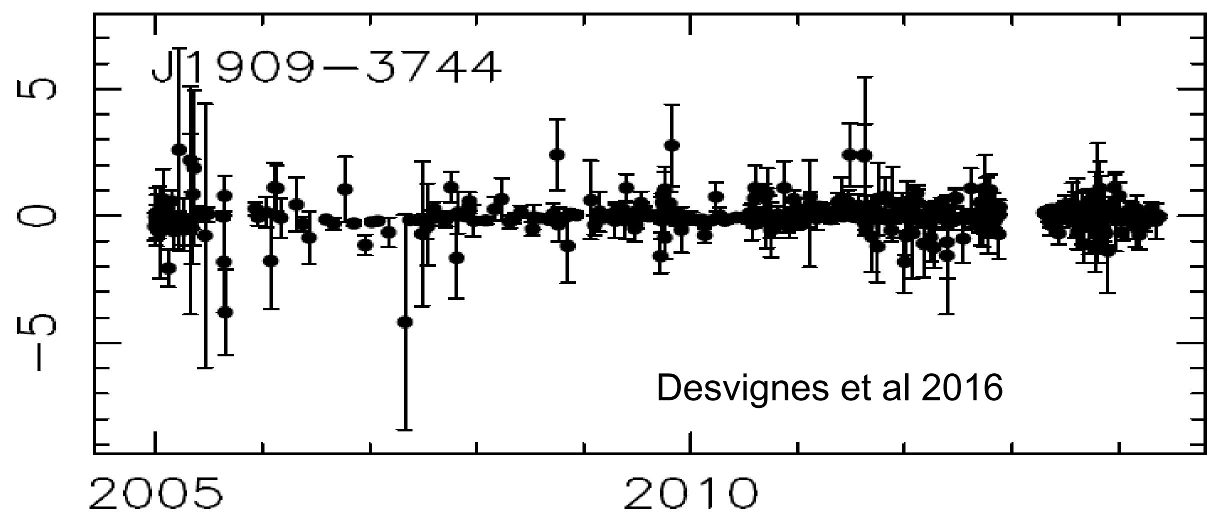

Red noise : Impact of planetary ephemerides

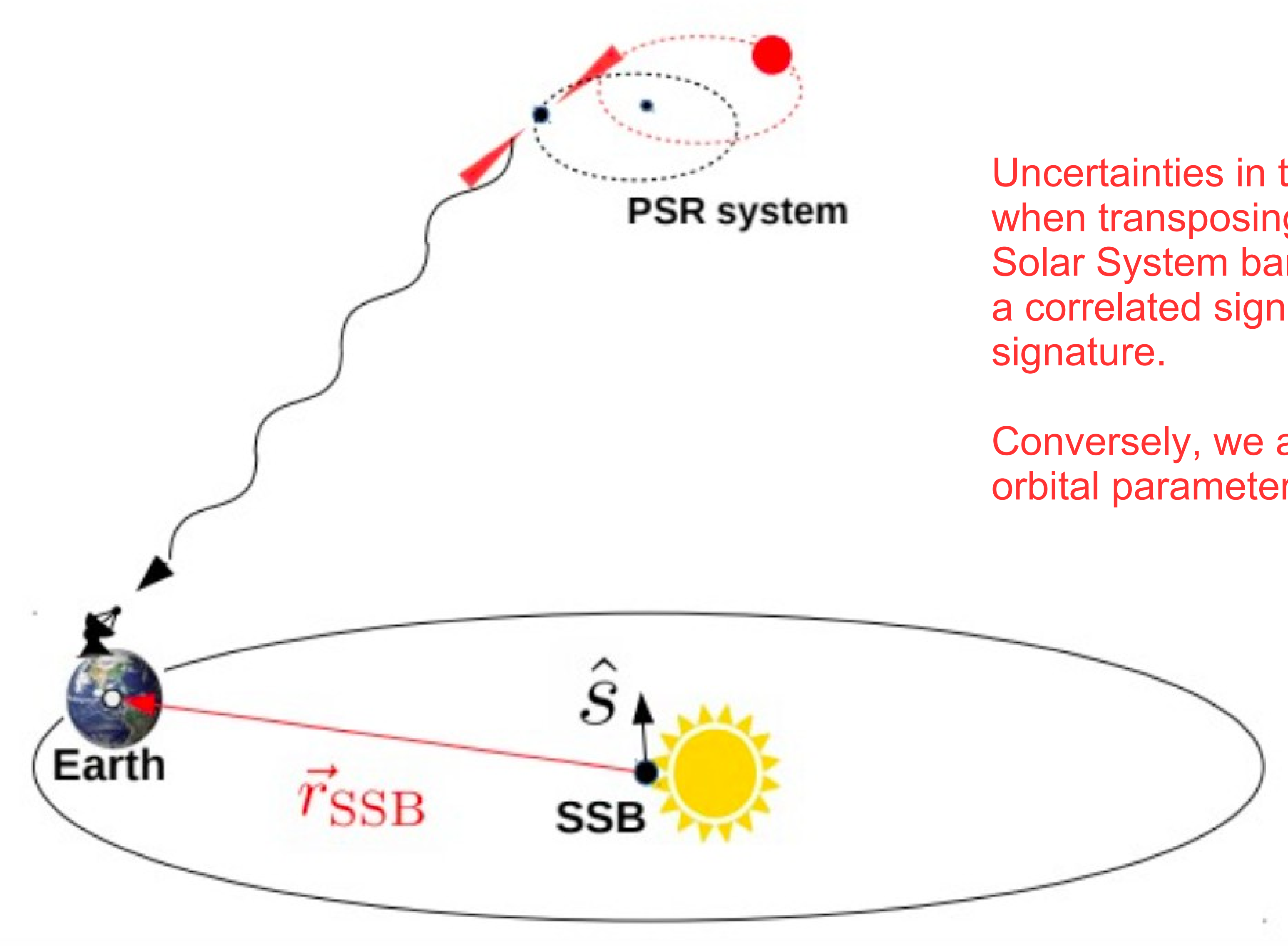

Uncertainties in the Römer delay when transposing to the Solar System barycentre induce a correlated signal with a dipole signature.

Conversely, we are sensitive to the orbital parameters of the planets!

Red noise : individual pulsar models

PSR J1600-3053

Chalumeau et al 2021 (EPTA)

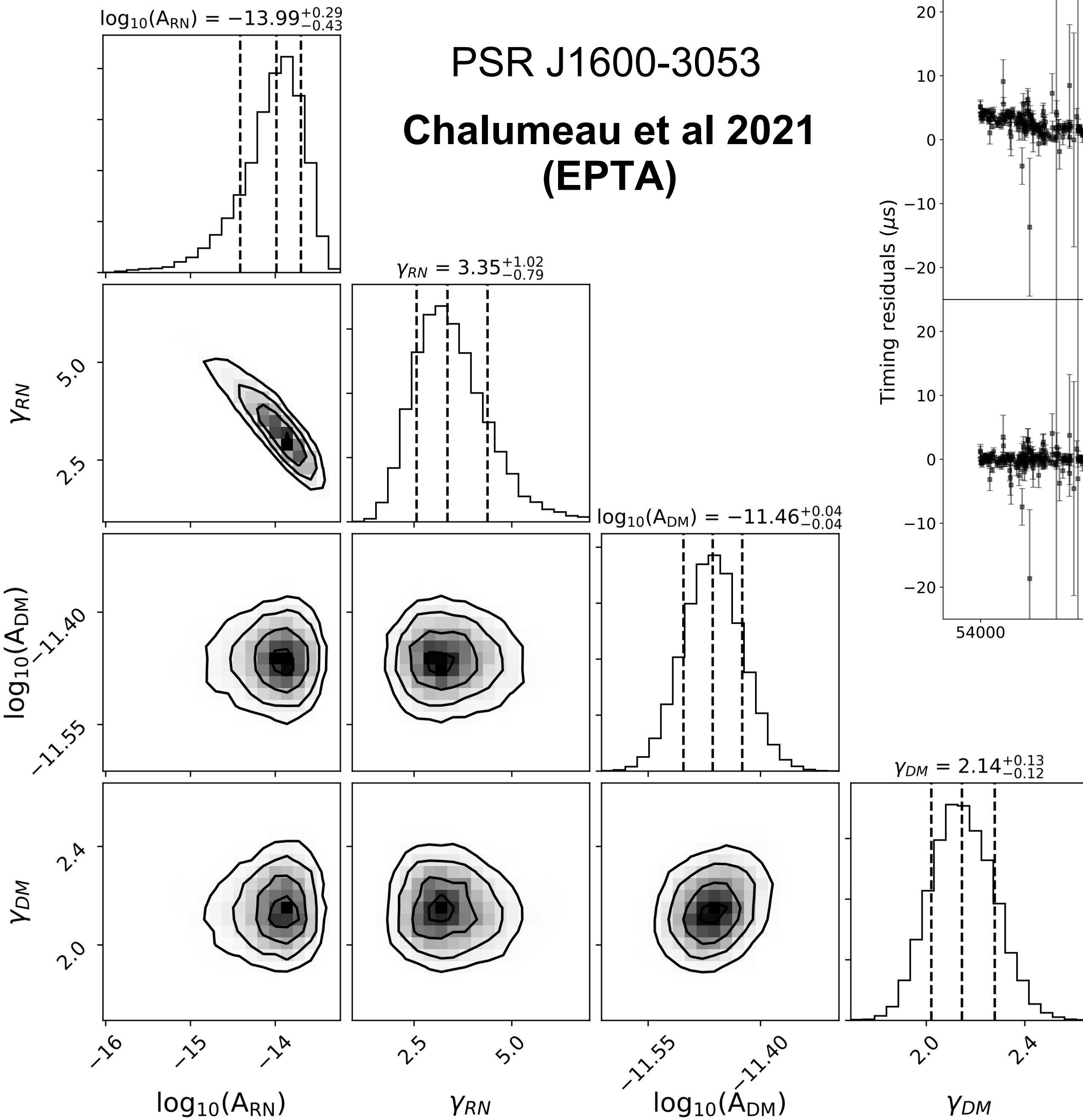

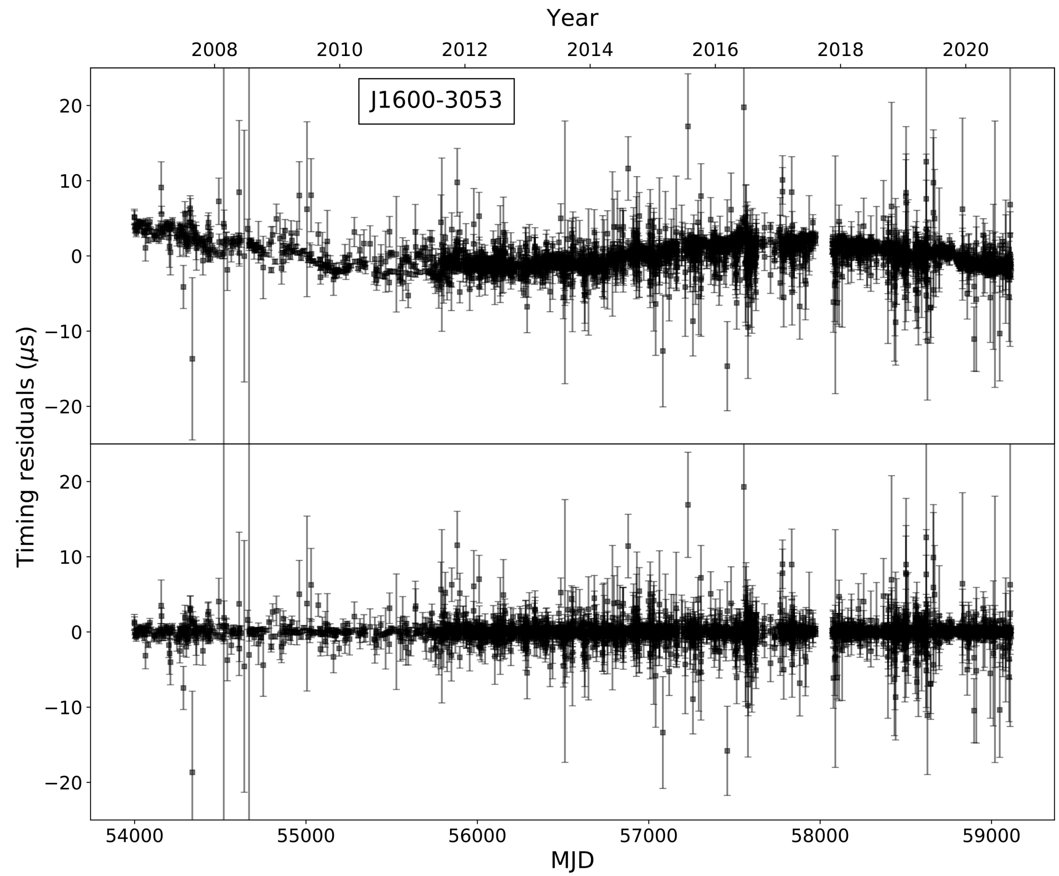

- **Spin noise**
- **DM chromatic noise**
- Scaterring noise
- Band noise
- System noise

+

Nb of freq bins
to characterise each

Pulsar Timing Arrays : principles

1) Describe the pulsar rotation in a reference frame co- moving with the pulsar

$$\nu(t) = \nu_0 + \dot{\nu}_0(t - t_0) + \frac{1}{2}\ddot{\nu}_0(t - t_0)^2 + \cdots$$

The observed parameters ν and ν are associated with the physical processes causing pulsars to spin down

2) Timing model

$$t_{SSB} = t_{topo} + \overbrace{t_{corr} - \delta D / f_{obs}^2 + \Delta_{R\odot} + \Delta_{\pi} + \Delta_{S\odot} + \Delta_{E\odot} + \Delta_R + \Delta_S + \Delta_E + \Delta_A}^{\boldsymbol{\tau}^{\mathrm{TM}}}$$

clock

dispersion

Solar System
Römer, parallax, Shapiro
and Einstein delays

binary system
Römer, Shapiro, Einstein
and Aberration delays

3) Full noise model

observed TOA $= \boldsymbol{\tau}^{\mathrm{TM}} + \overbrace{\boldsymbol{\tau}^{\mathrm{WN}} + \boldsymbol{\tau}^{\mathrm{SN}} + \boldsymbol{\tau}^{\mathrm{DM}} + \boldsymbol{\tau}^{\mathrm{CN}}}^{\text{Noise model}} + \boldsymbol{\tau}^{\mathrm{GW}}$

Timing Model (deterministic)

meas. (white) noise

pulsar spin (red) noise

DM (red) noise

Clock Ephem. Astroph. (red) noise

GWB (red) noise

The life cycle of supermassive binary black holes

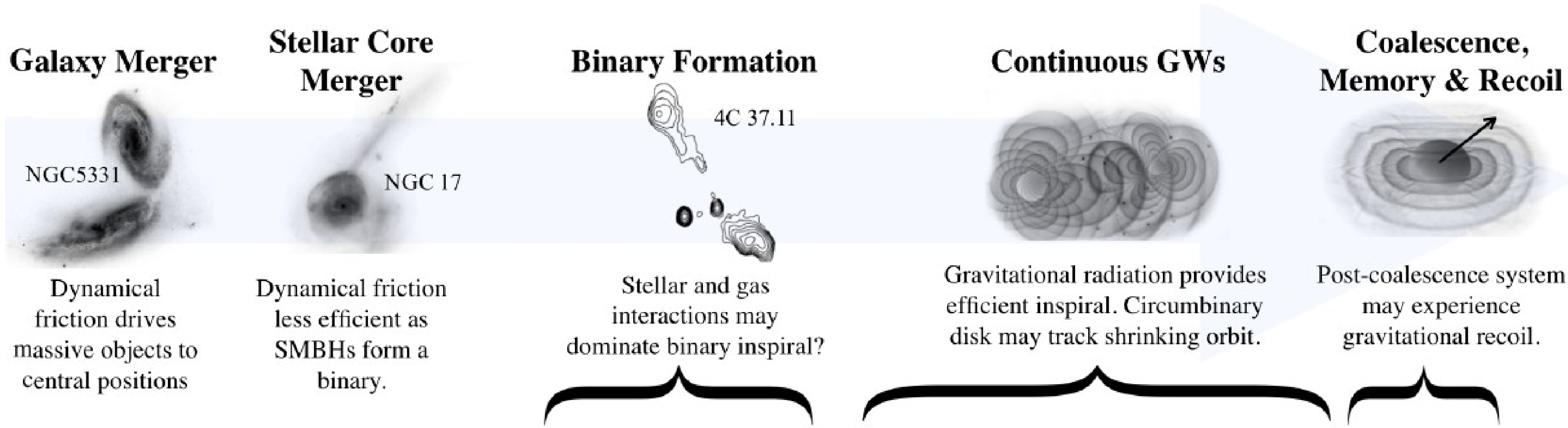

Do we have a chance to get a detection with the PTA technique in a reasonable time ?

How can we characterize the detected signal ?

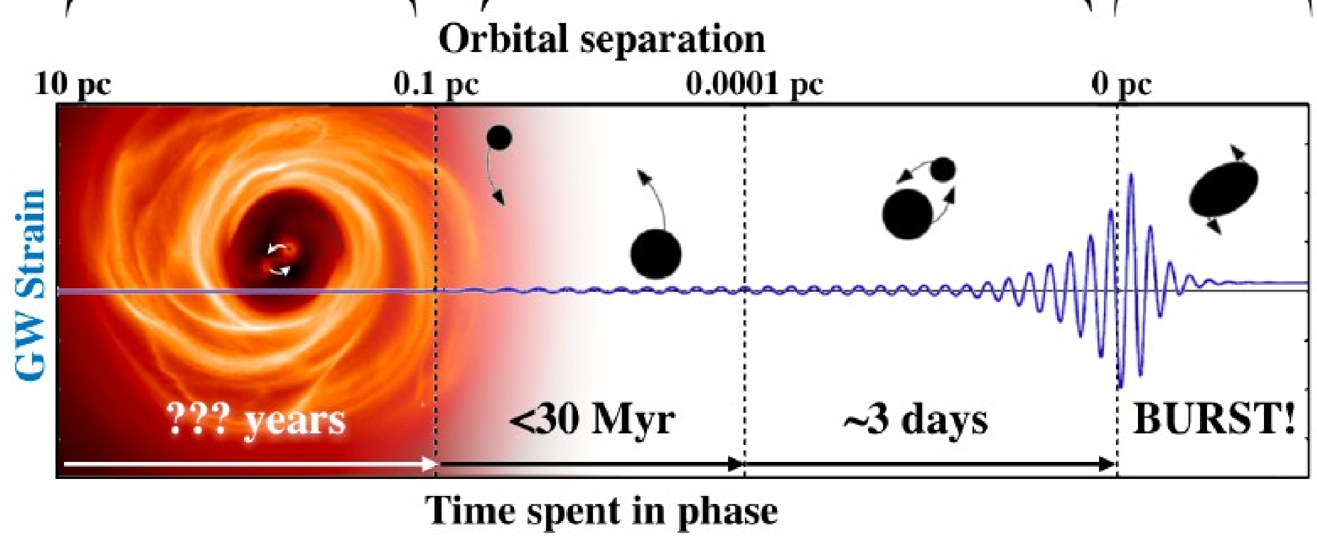

Burke-Spolaor 2018

monochromatic PTA regime

Population synthesis ingredients

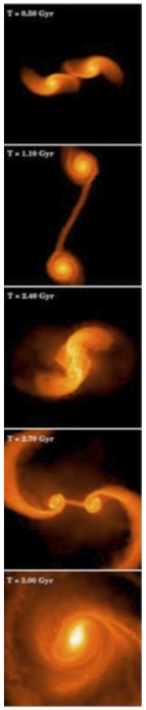

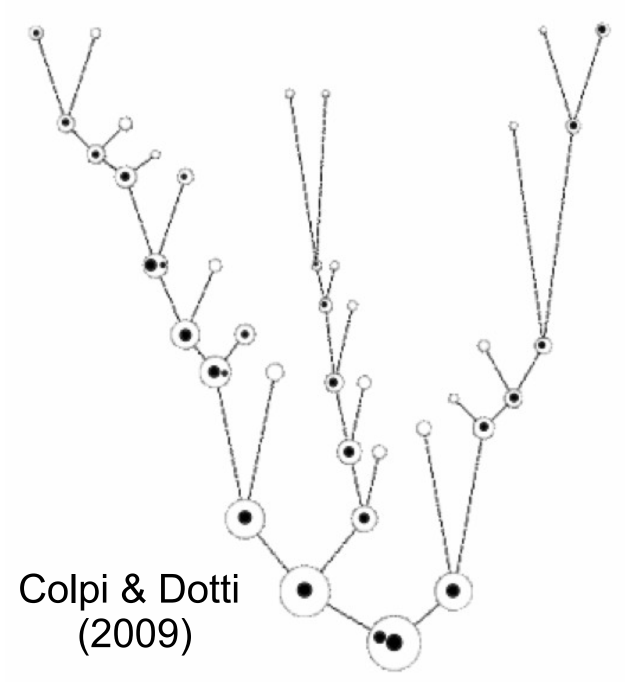

Colpi & Dotti (2009)

Reines & Volonteri (2015)

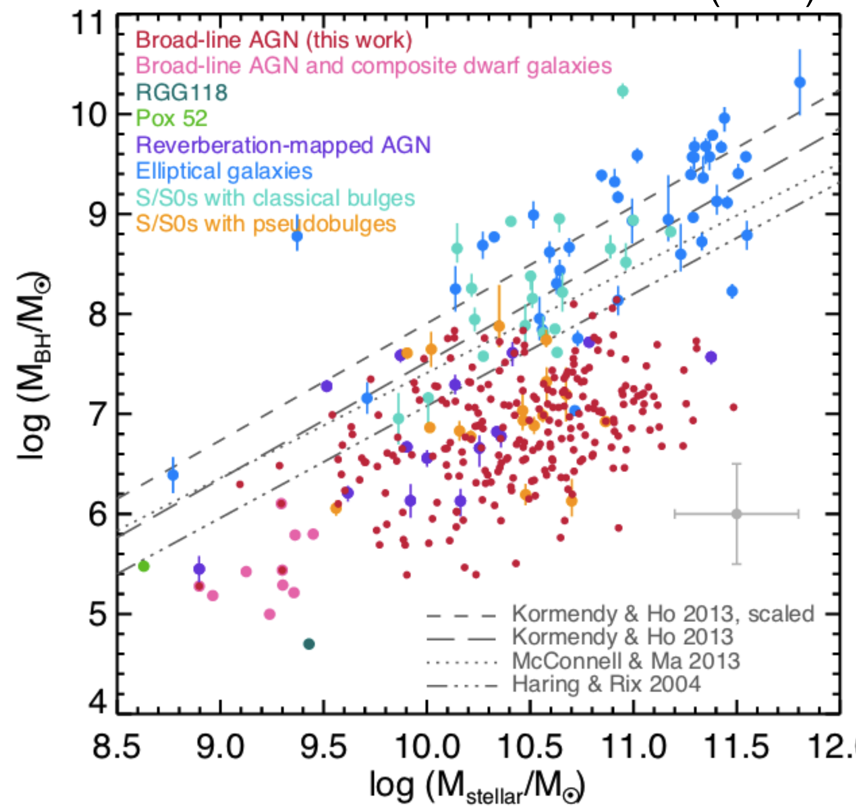

Merger trees from cosmological N-body simulations (Illustris, TNG, EAGLE, Horizon-AGN, SIMBA ...)

Bulge to BH mass ratio from galaxies dynamical studies

Add dynamical friction with stars and gas to migrate the BHs towards the center

Three body interaction with stars from the loss cone region (when binary orbital velocity > stars)

Population synthesis ingredients

Last parsec problem:

the BH pair empties its environment and stops losing energy.

→ do most of the pairs reach the gravitational regime within a Hubble time ?

A few answers:

- massive BH triplets (Bonetti et al 2018),
- triaxial potential/density of the nuclei refilling the loss-cone (Vasiliev et al 2015),
- circumbinary accretion disk (Tang et al 2017)
- Continuous accretion of clumpy cold gas on to the nucleus (Goicovic et al 2018)
- a large population of stalled binaries at low frequencies (Dvorkin&Barausse 2017)

Population of SMBBH : contribution from background & individual sources

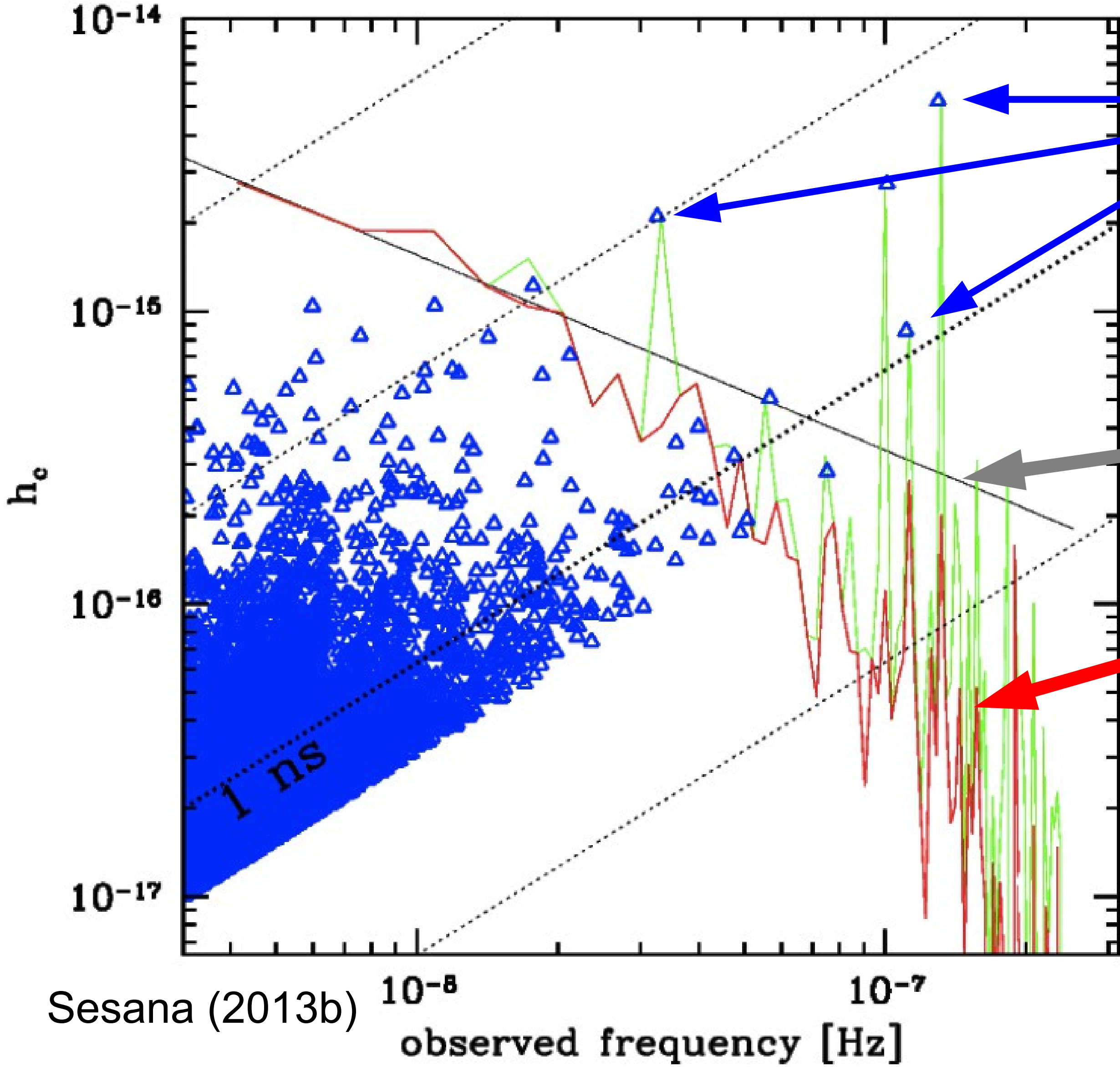

Sesana (2013b)

« resolvable » individual sources

stochastic background ~ f $^{-2/3}$

contribution from unresolved sources

Hypothesis :

- circular orbits
- all the population reaches the sub-pc GW emission regime

+ uncertainties about :

fusion rate
BH – host galaxy mass relation
time to coalescence

stochastic background ~ f $^{-2/3}$

$$h_c^2(f) = \int_0^\infty dz \int_0^\infty d\mathcal{M} \frac{d^3N}{dz d\mathcal{M} d\ln f_r} h^2(f_r) \longrightarrow h_c(f) = A \left(\frac{f}{\mathrm{yr}^{-1}}\right)^{-2/3}$$

(Phinney 2001)

Pulsar Timing Arrays : principles

GW induced timing residuals (simulated data) from Burke-Spolaor (2015)

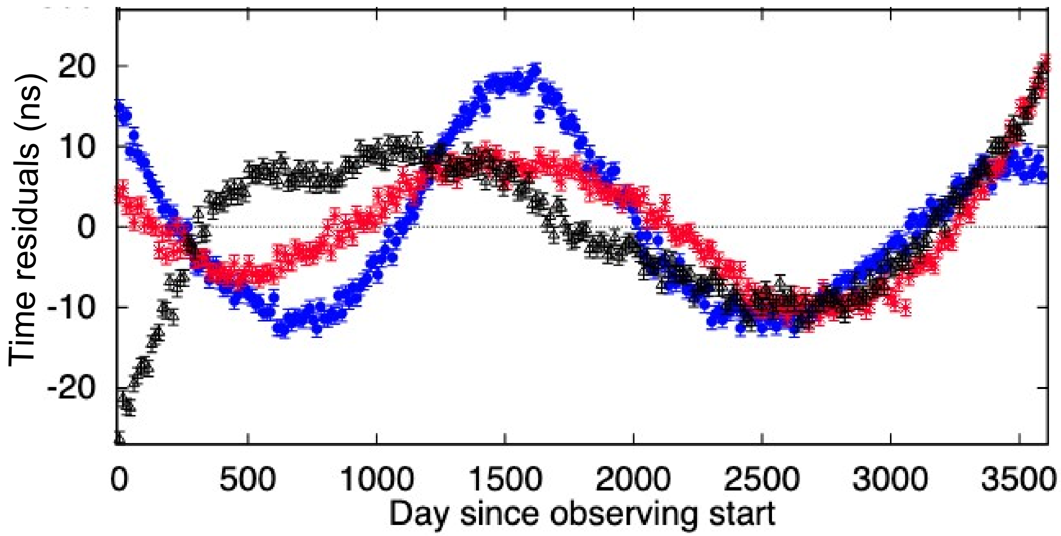

(a) Gravitational Wave Background

PSR J0437–4715
PSR J1012+5307
PSR J1713+0747

(a) a GWB with $h_c = 10^{-15}$ and $\alpha = -2/3$

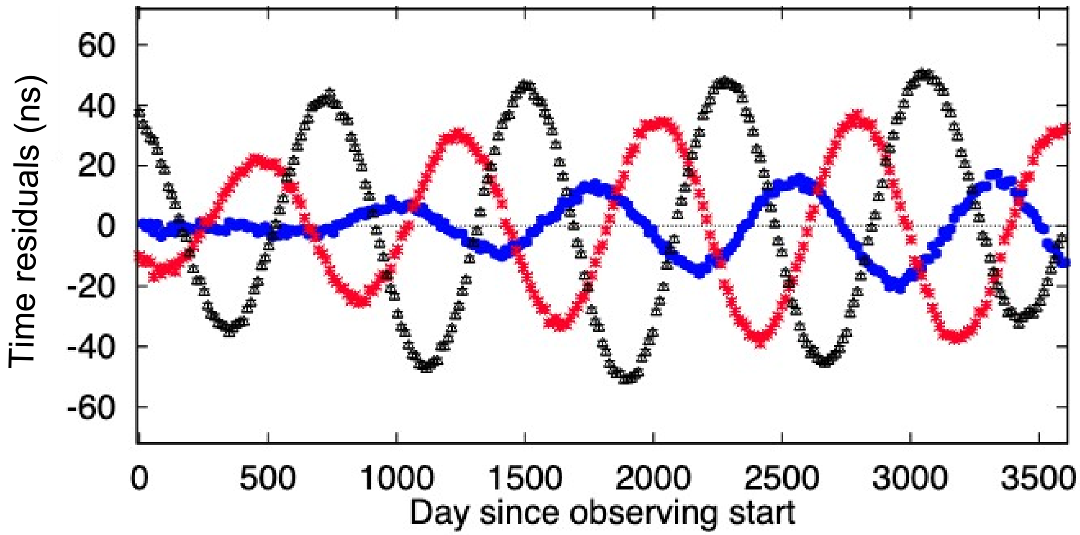

(b) Continuous Wave

(b) a continuous wave
(injected in the same sky location)
from an equal-mass 10^9 M BSMBH
at redshift z = 0.01.

distortion from a perfect sinusoid is caused by the lower-frequency pulsar term

Searching for individual sources

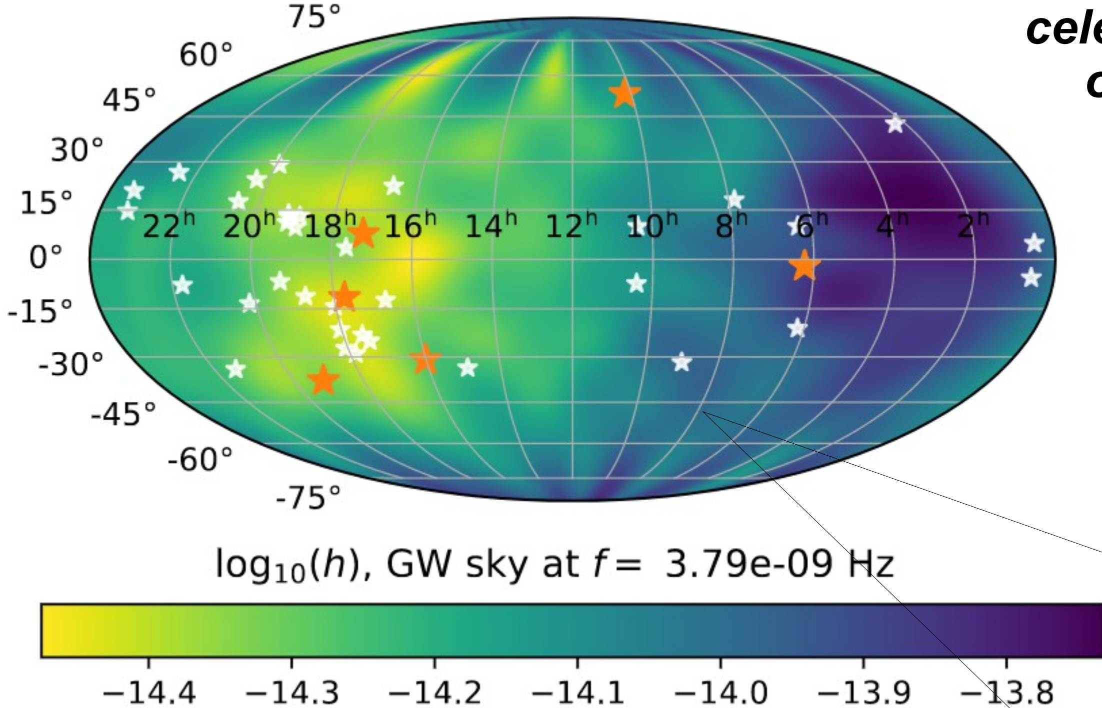

The sensitivity of the pulsar array depends on the position on the celestial sphere and on the distribution of pulsar pair angular separations

Mingarelli et al 2017
Sky sensitivity map
from EPTA-2015 at 3.8 nHz

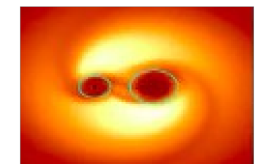

individual Sources ?

(α,δ) GW spectrum

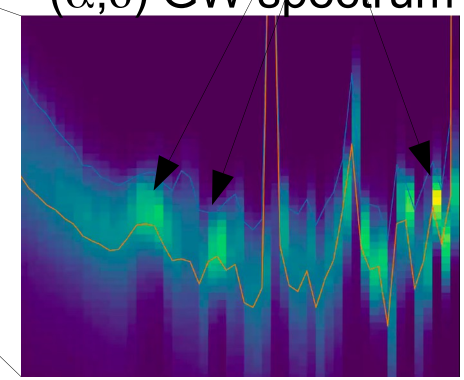

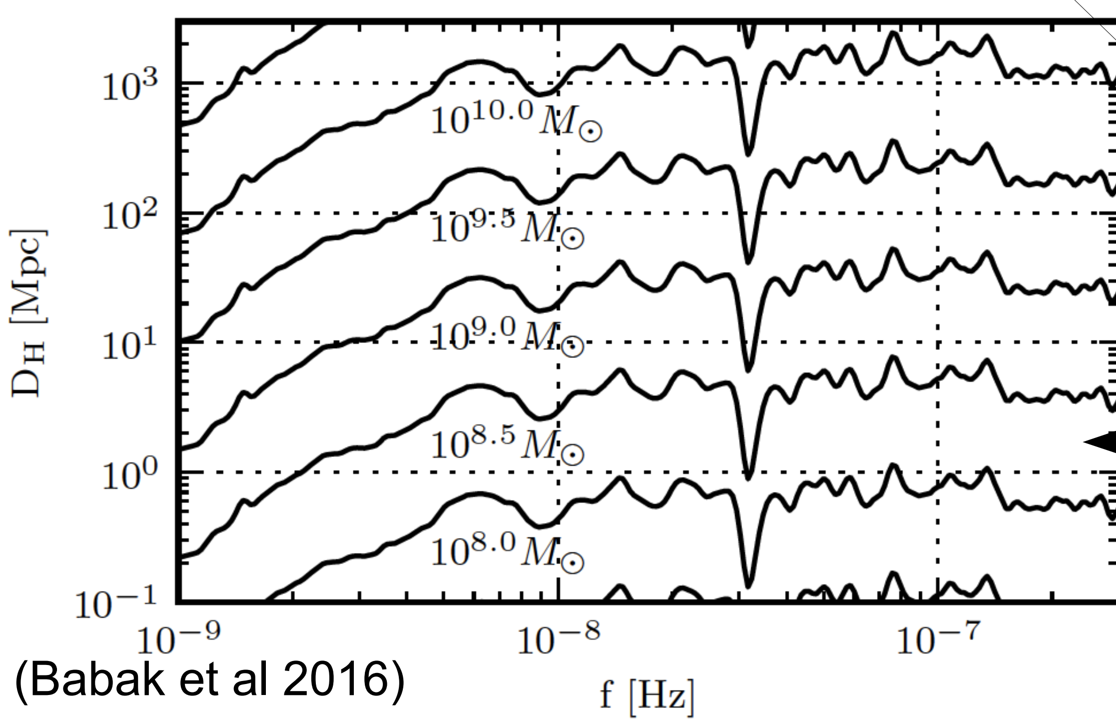

(Babak et al 2016)

EPTA-2015 (Babak et al 2016) :
hc < 1.1×10^{-14} at 10 nHz

On can exclude the presence of a SMBHB with a « chirp mass »

$\mathcal{M}c > 10^9\ M_\odot$ up to 25Mpc

$\mathcal{M}c > 3\ 10^9\ M_\odot$ up to 200 Mpc

Searching for individual sources

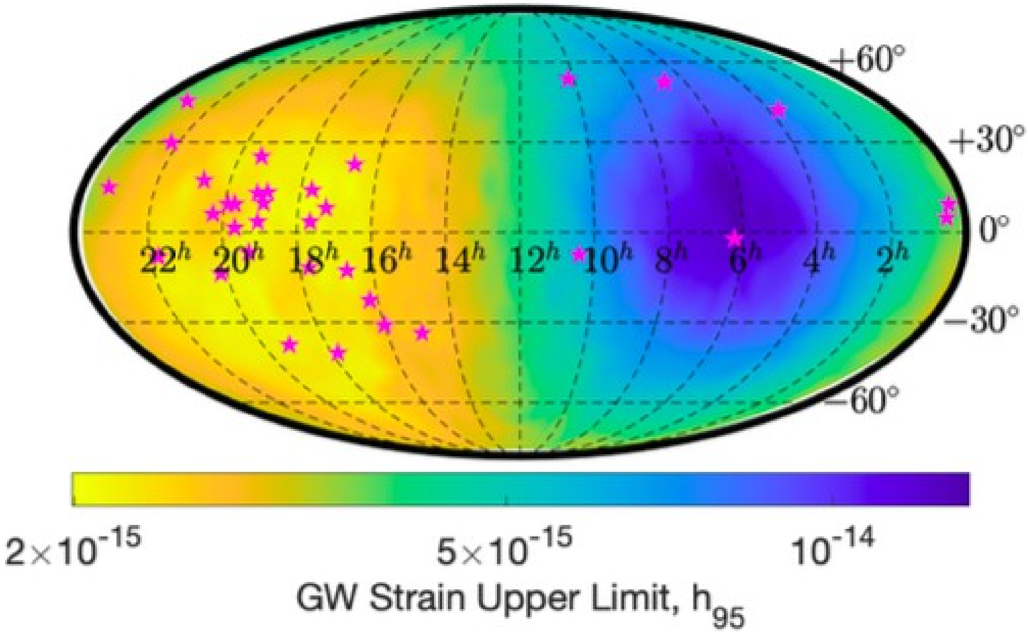

The sensitivity of the pulsar array depends on the position on the celestial sphere and on the distribution of pulsar pair angular separations

Arzoumanian et al 2021
Sky sensitivity map
from NANOGrav-11yr at 8 nHz
hc < 7.3×10^{-15}

No equal mass SMBHB
with chirp mass M > 1.6×10^{9} M
in the Virgo Cluster
(Aggarwal et al 2019)

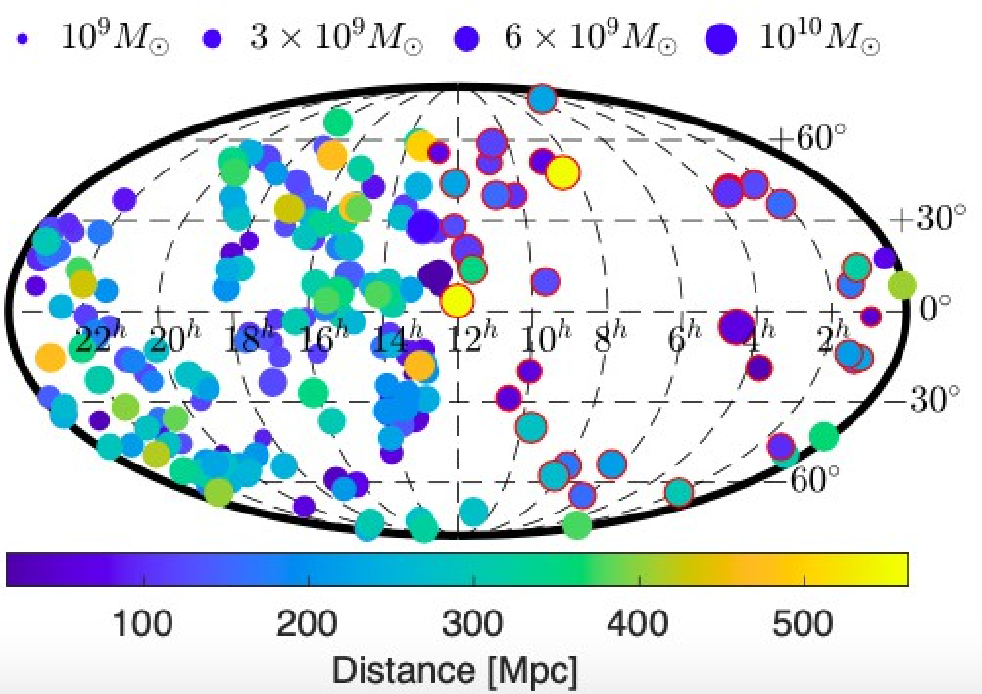

Place constraints on putative SMBHBs in nearby massive galaxies (Arzoumanian et al 2021)

44,000 galaxies in the local universe (up to redshift   0.05) and populated them with hypothetical binaries

216 galaxies with dynamical mass within NANOGrav's sensitivity volume

+ constraints on their chirp mass and mass ratio

OJ 287 as a SMBH binary candidate

(discovered in 1988 by Sillanpää et al)

also NGC5548, NGC4151, Mrk231

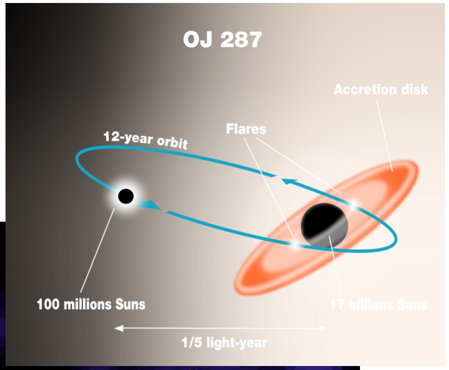

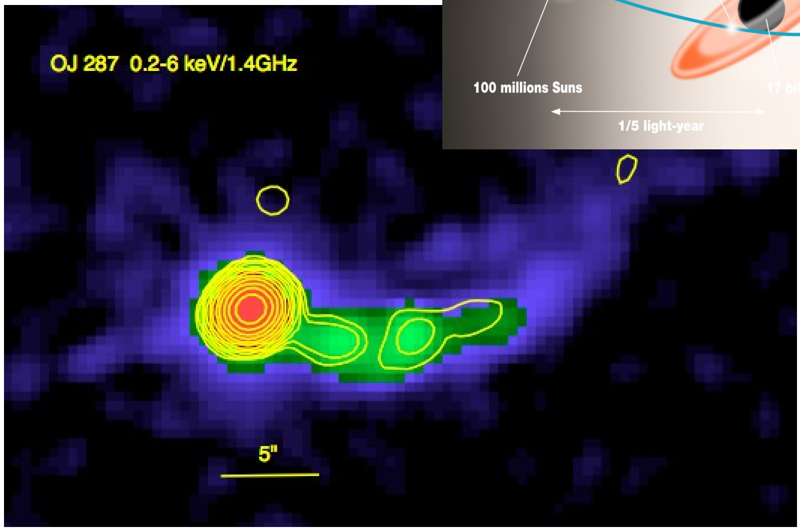

Zhu et al 2018 computed the probability distribution of the gravitional wave background amplitude assuming those objects are true SMBHBs

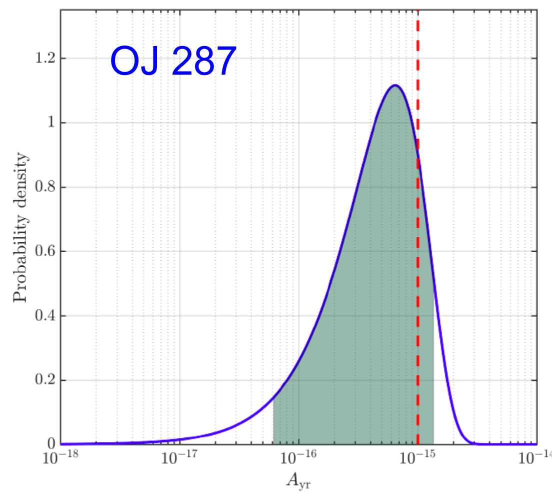

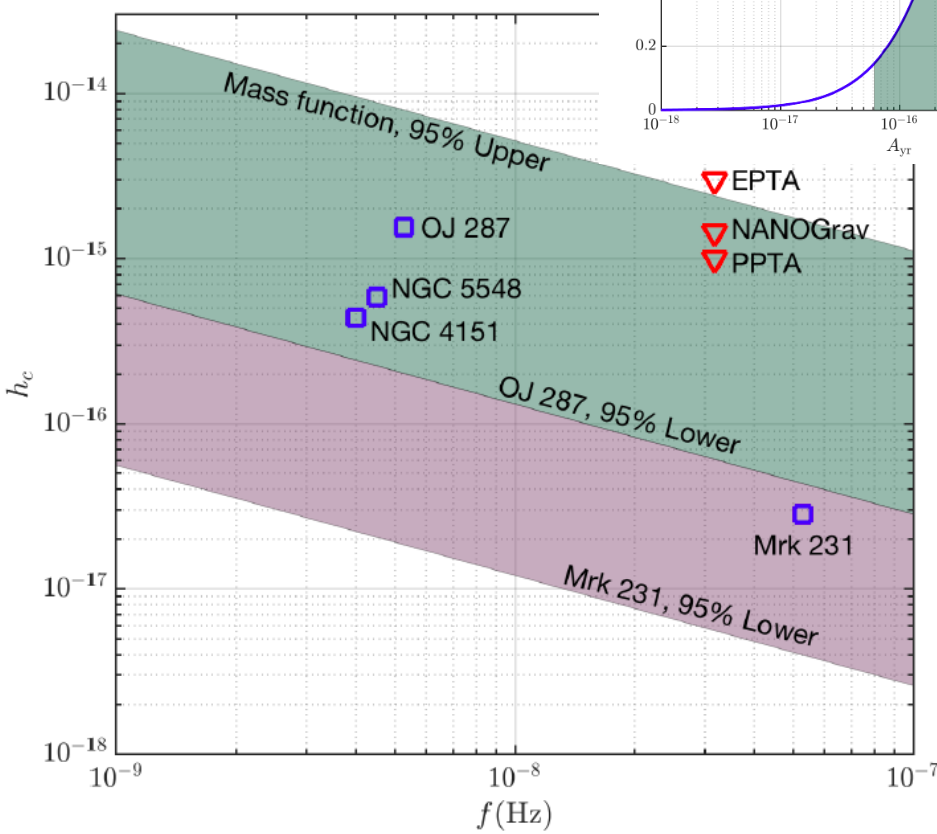

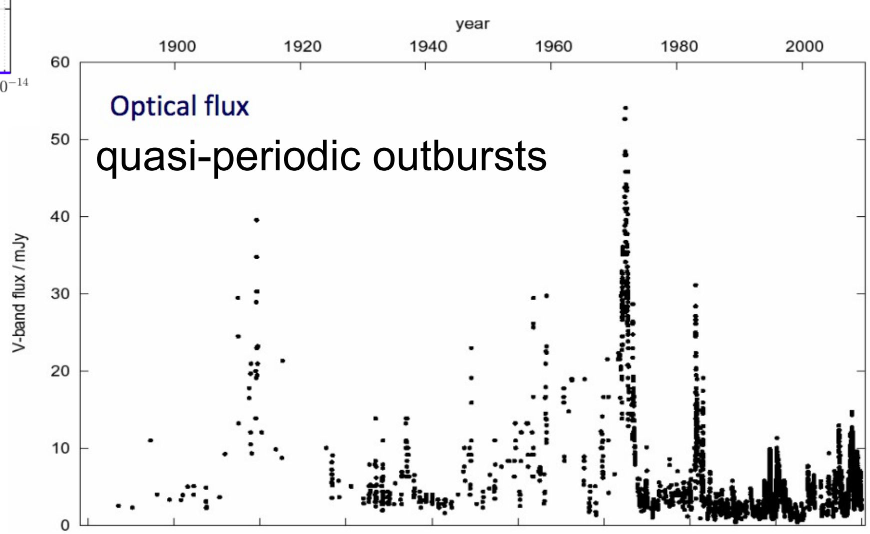

OJ 287
~12 yrs period
18 x 10^9 solar masses
0.663 eccentricity
z =0.3

Ciprini et al 2016
Valtonen et al 2008

Periodic variability of quasars and AGNs (Graham et a 2015, Sesana et al 2018)

Binarity induces periodic material streaming from the cavity edge onto the binary, and hence luminosity periodicity, better detected in X-ray and UV

Catalina Real-time Transient Survey (CRTS – 250,000 QSOs)
→ 111 periodic sources (P < 6 yrs ; Graham et al 2015)

Palomar Transient Factory (OTF – 35,000 QSOs)
→ 33 periodic sources (Charisi et al 2016)

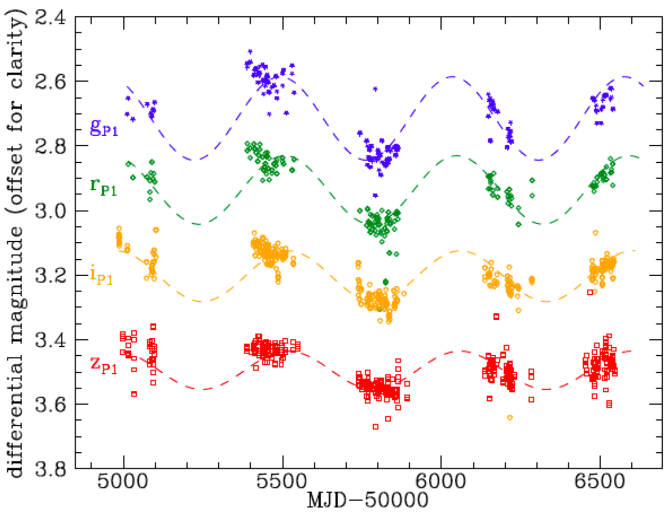

Liu et al 2015 (Catalina)
PSO J334.2028+01.4075
Pobs = 542 days
$\log(M_{BH}) = 9.97$
Q = 0.05-0.25

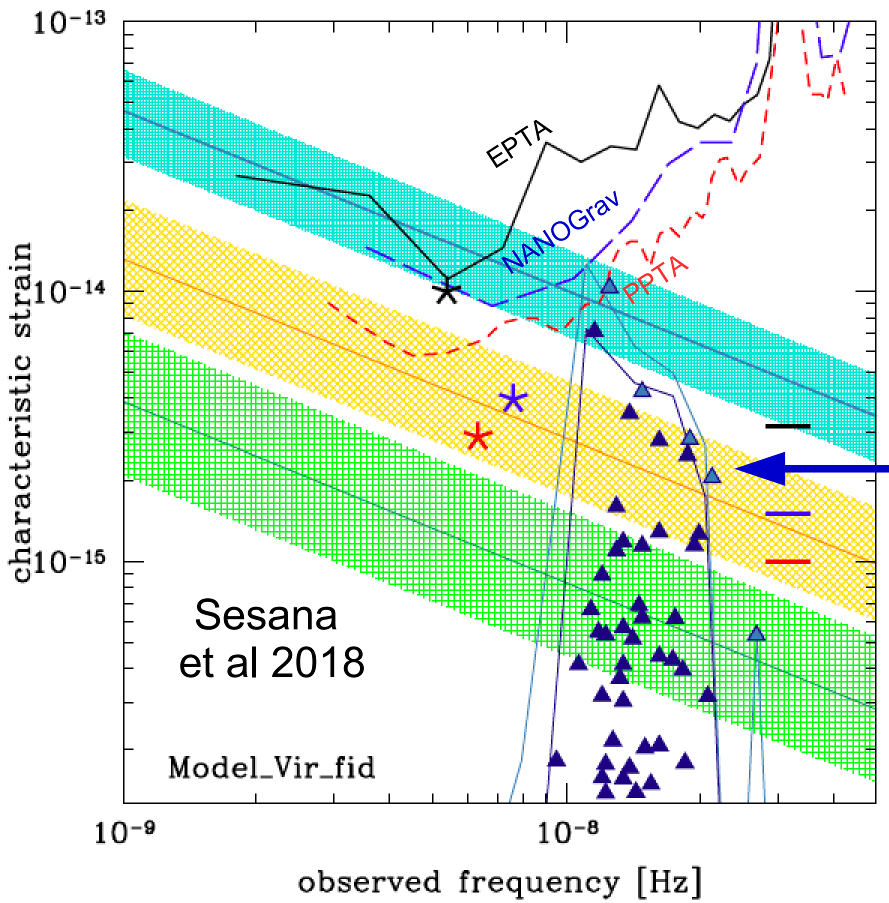

Sesana et al 2018 :
compute SMBHB merger rate for periodic sources and construct the expected gravitational wave background

Periodic QSO candidates in tension with PTA results and population models (mainly high z >1.3)

The stochastic gravitational wave background (SGWB): detection vs upper limit

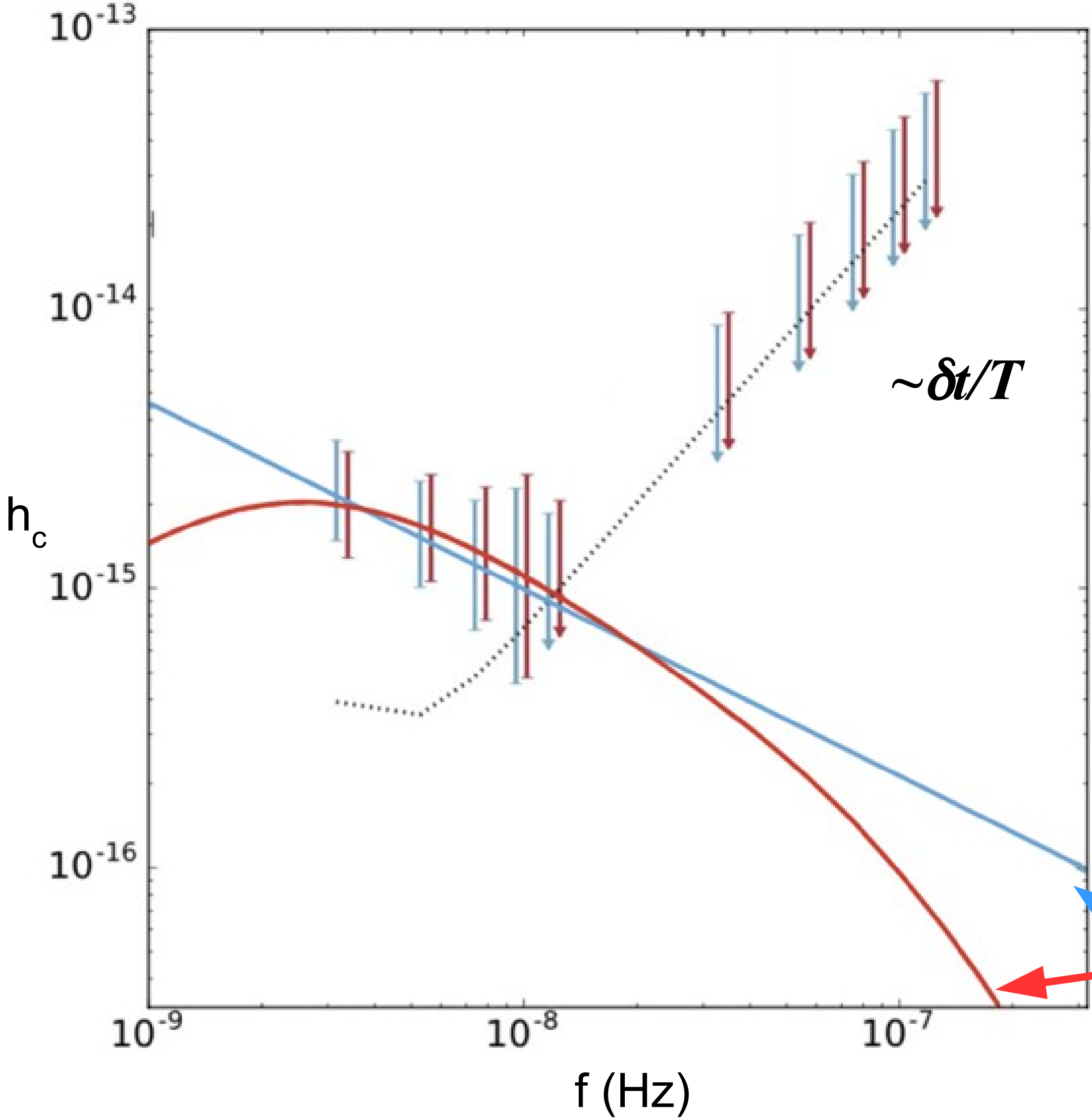

$$h_c(f) = A\left(\frac{f}{\mathrm{yr}^{-1}}\right)^{-2/3}$$

Expected spectrum for a population of super massive black hole binaries

purely circular orbits, isolated pairs

including eccentricity, stellar hardening, ...

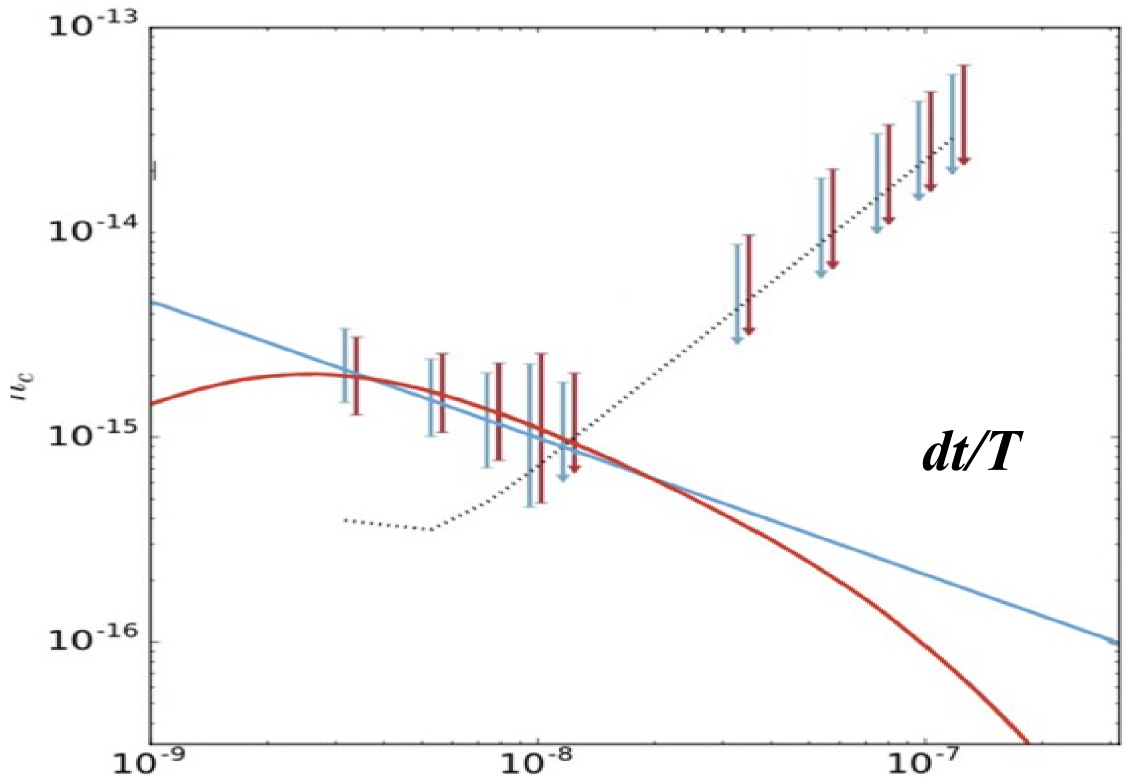

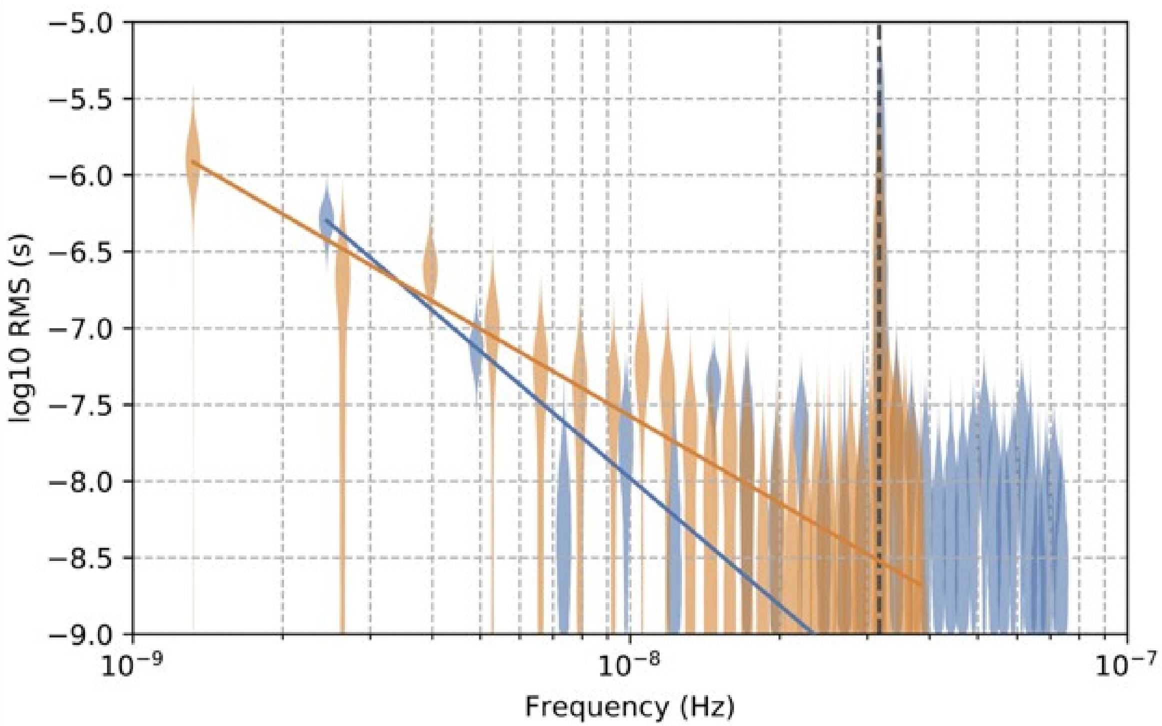

Bayes factor diagnostic (EPTA):

ID	Model	lg10BF ENTERPRISE	lg10BF FORTYTWO
0	PSRN	0	0
1	PSRN + CURN	3.1 ± 0.05	3.6 ± 0.1
2	PSRN + GWB	2.73 ± 0.03	3.2 ± 0.1
3	PSRN + CLK	0.62 ± 0.03	0.8 ± 0.1
4	PSRN + EPH	2.06 ± 0.04	2.1 ± 0.1
5	PSRN + CURN + GWB	2.89 ± 0.03	3.7 ± 0.3
6	PSRN + CURN + CLK	3.06 ± 0.03	3.4 ± 0.1
7	PSRN + CURN + EPH	2.99 ± 0.03	3.4 ± 0.2

A first detection ?

EPTA result :
6 « best » pulsars, 14-25 years
(Chen et al 2021a)

NANOGrav result :
47 pulsars, 12.5 years
(Arzoumanian et al 2020)

The PTA common red noise signal vs SMBHB population models

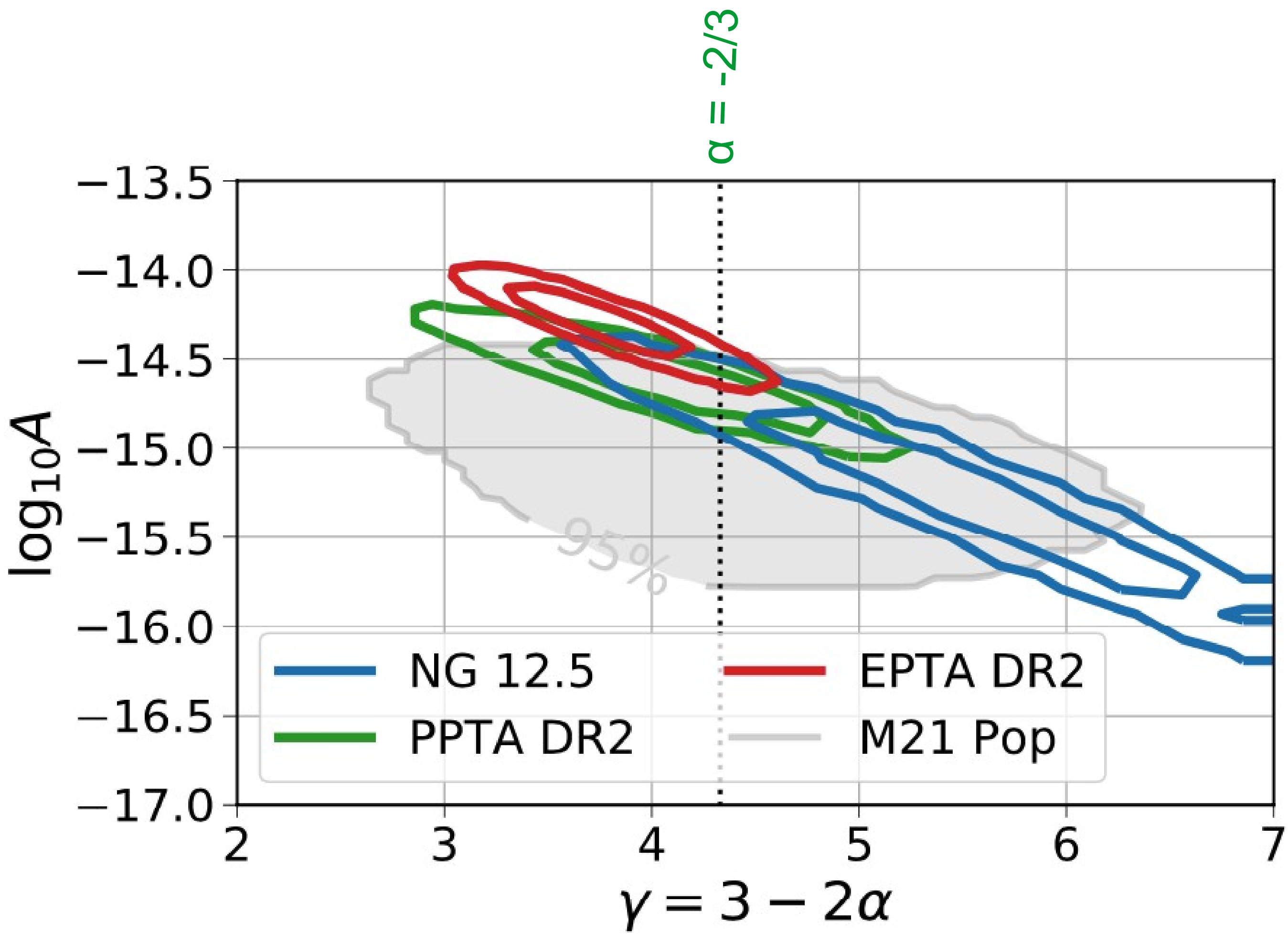

Antoniadis et al 2022

Arzoumanian et al 2020
Chen et al 2021
Goncharov et al 2021

Comparing with the predictions of astrophysical models (Middleton et al 2021)

$$h_c(f) = A\left(\frac{f}{\mathrm{yr}^{-1}}\right)^{-2/3}$$

→

high merger rate densities

short merger timescales

high normalization
for BH-bulge mass relation

Population of SMBBH : contribution from background & individual sources

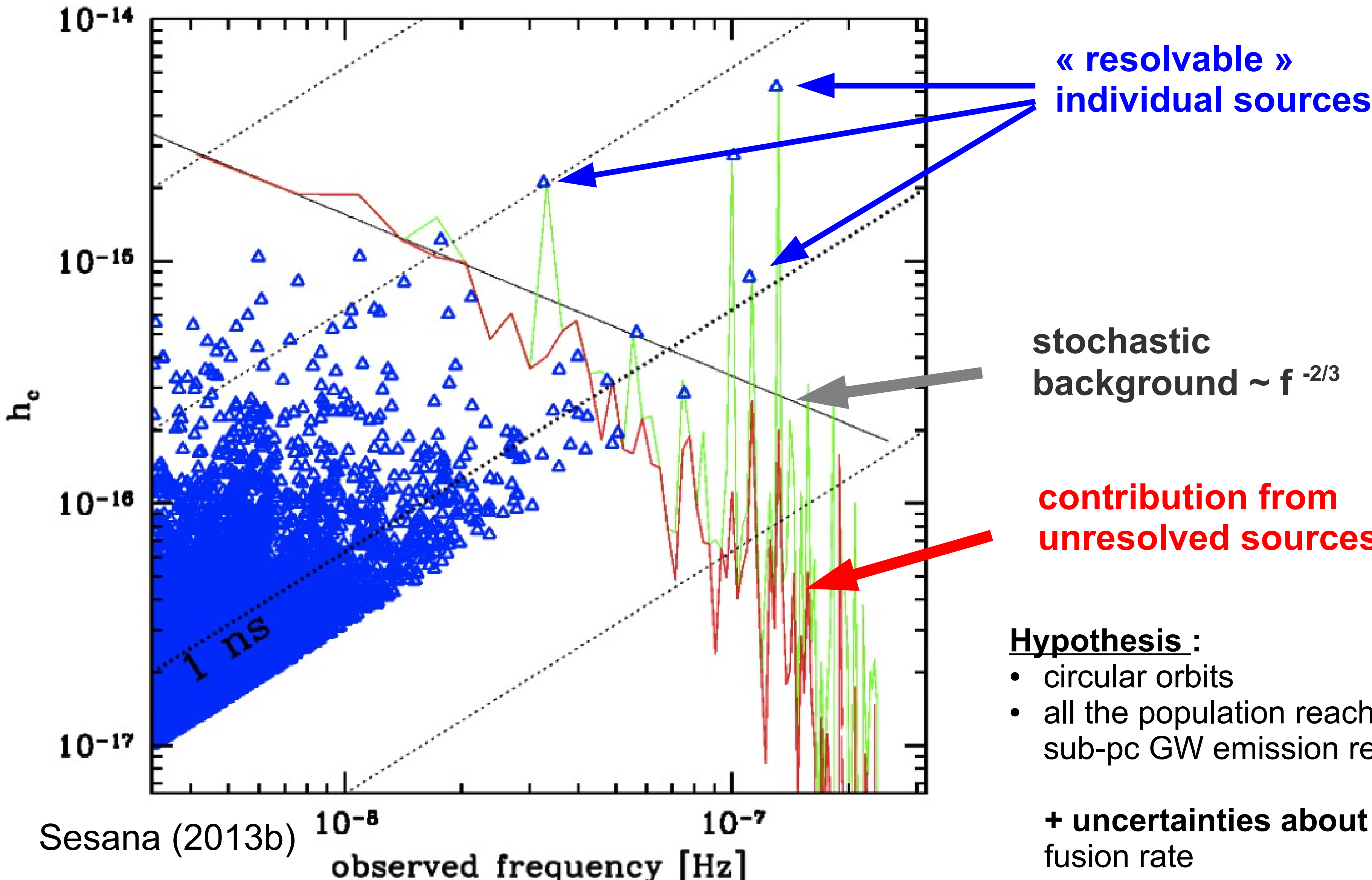

Sesana (2013b)

Hypothesis :

- circular orbits
- all the population reaches the sub-pc GW emission regime

+ uncertainties about :
fusion rate
BH – host galaxy mass relation
time to coalescence

stochastic background ~ f $^{-2/3}$

$$h_c^2(f) = \int_0^\infty dz \int_0^\infty d\mathcal{M} \, \frac{d^3N}{dz\, d\mathcal{M}\, d\ln f_r} h^2(f_r) \longrightarrow h_c(f) = A \left(\frac{f}{\mathrm{yr}^{-1}} \right)^{-2/3}$$

(Phinney 2001)

A more realistic scenario :

+ eccentricity

+ interactions with stars and gas

+ spin/orbite coupling

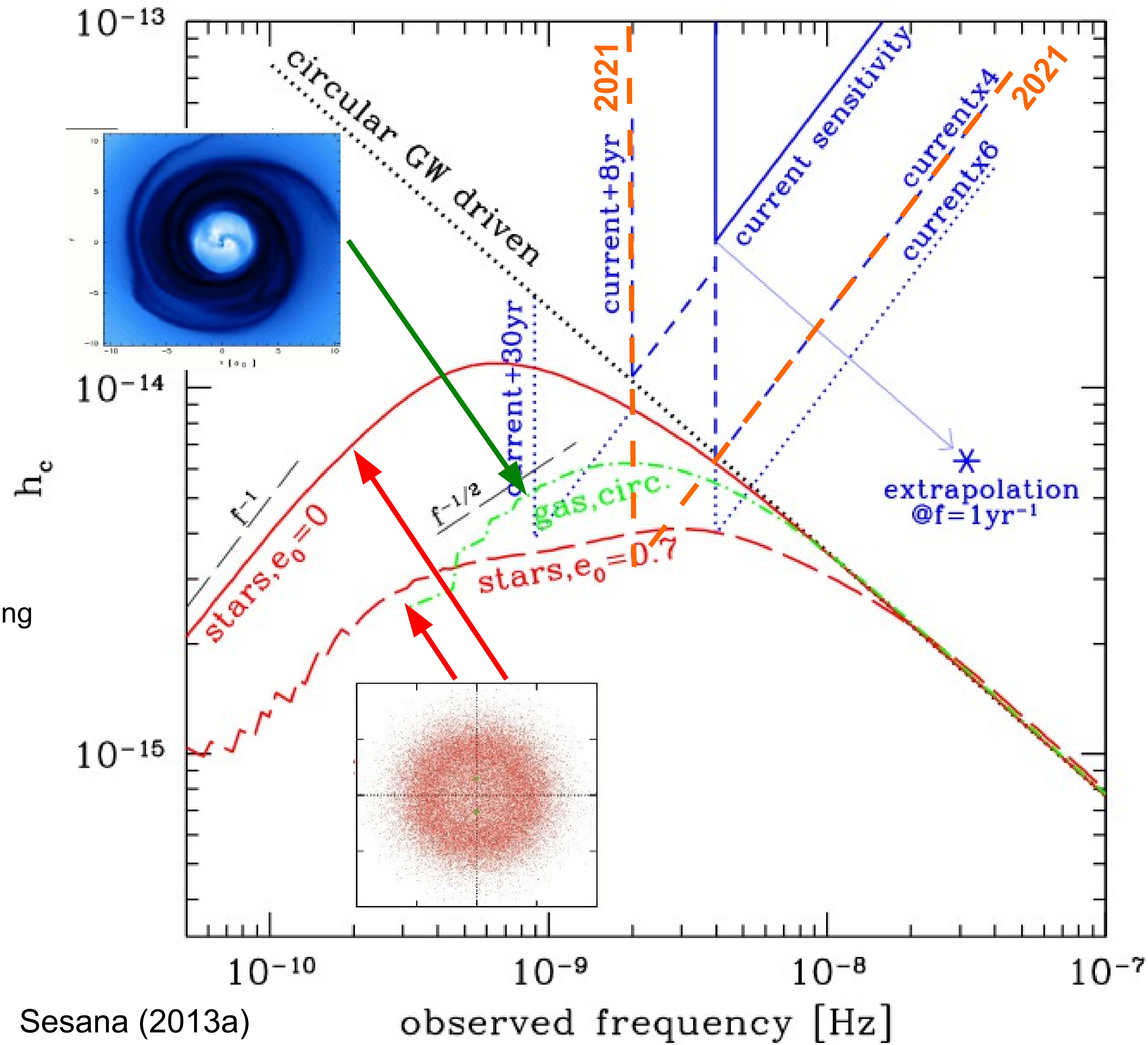

Sesana (2013a)

Constraints on astrophysical models

Chen et al 2019
EPTA – population synthesis

parameter	description	standard	extended
Φ_0	GSMF norm	-2.8 ± 0.3	-2.8 ± 0.3
Φ_I	GSMF norm redshift evolution	-0.25 ± 0.22	-0.25 ± 0.22
$\log_{10}M_0$	GSMF scaling mass	11.25 ± 0.2	11.25 ± 0.2
α_0	GSMF mass slope	-1.25 ± 0.17	-1.25 ± 0.17
α_I	GSMF mass slope redshift evolution	0 ± 0.15	0 ± 0.15
f_0	pair fraction norm	[0.02,0.03]	[0.01,0.05]
α_f	pair fraction mass slope	[-0.2,0.2]	[-0.5,0.5]
β_f	pair fraction redshift slope	[0.6,1]	[0,2]
γ_f	pair fraction mass ratio slope	[-0.2,0.2]	[-0.2,0.2]
τ_0	merger time norm	[0.1,2]	[0.1,10]
α_τ	merger time mass slope	[-0.2,0.2]	[-0.5,0.5]
β_τ	merger time redshift slope	[-2,1]	[-3,1]
γ_τ	merger time mass ratio slope	[-0.2,0.2]	[-0.2,0.2]
$\log_{10}M_*$	$M_{\rm bulge}-M_{\rm BH}$ relation norm	8.17 ± 0.33	8.17 ± 0.33
α_*	$M_{\rm bulge}-M_{\rm BH}$ relation slope	1 ± 0.1	1 ± 0.1
ε	$M_{\rm bulge}-M_{\rm BH}$ relation scatter	[0.3,0.5]	[0.2,0.5]
e_0	binary eccentricity	[0.01,0.99]	[0.01,0.99]
$\log_{10}\zeta_0$	stellar density factor	[-2,2]	[-2,2]

Galaxy stellar mass function

Pair fraction

Merger timescale

M_{bulge} -M_{BH} relation

Eccentricity and stellar density

Constraints on astrophysical models

Chen et al 2019
EPTA – population synthesis

parameter	description	standard	extended
	Galaxy stellar mass function		
Φ_0	GSMF norm	-2.8 ± 0.3	-2.8 ± 0.3
Φ_I	GSMF norm redshift evolution	-0.25 ± 0.22	-0.25 ± 0.22
$\log_{10}M_0$	GSMF scaling mass	11.25 ± 0.2	11.25 ± 0.2
α_0	GSMF mass slope	-1.25 ± 0.17	-1.25 ± 0.17
α_I	GSMF mass slope redshift evolution	0 ± 0.15	0 ± 0.15
	Pair fraction		
f_0	pair fraction norm	[0.02,0.03]	[0.01,0.05]
α_f	pair fraction mass slope	[-0.2,0.2]	[-0.5,0.5]
β_f	pair fraction redshift slope	[0.6,1]	[0,2]
γ_f	pair fraction mass ratio slope	[-0.2,0.2]	[-0.2,0.2]
	Merger timescale		
τ_0	merger time norm	[0.1,2]	[0.1,10]
α_τ	merger time mass slope	[-0.2,0.2]	[-0.5,0.5]
β_τ	merger time redshift slope	[-2,1]	[-3,1]
γ_τ	merger time mass ratio slope	[-0.2,0.2]	[-0.2,0.2]
	M_{bulge} -M_{BH} relation		
$\log_{10}M_*$	$M_{\rm bulge}-M_{\rm BH}$ relation norm	8.17 ± 0.33	8.17 ± 0.33
α_*	$M_{\rm bulge}-M_{\rm BH}$ relation slope	1 ± 0.1	1 ± 0.1
ε	$M_{\rm bulge}-M_{\rm BH}$ relation scatter	[0.3,0.5]	[0.2,0.5]
	Eccentricity and stellar density		
e_0	binary eccentricity	[0.01,0.99]	[0.01,0.99]
$\log_{10}\zeta_0$	stellar density factor	[-2,2]	[-2,2]

Case of no-detection

Strain limit : $A(f=\mathrm{yr}^{-1})=1\times10^{-15}$

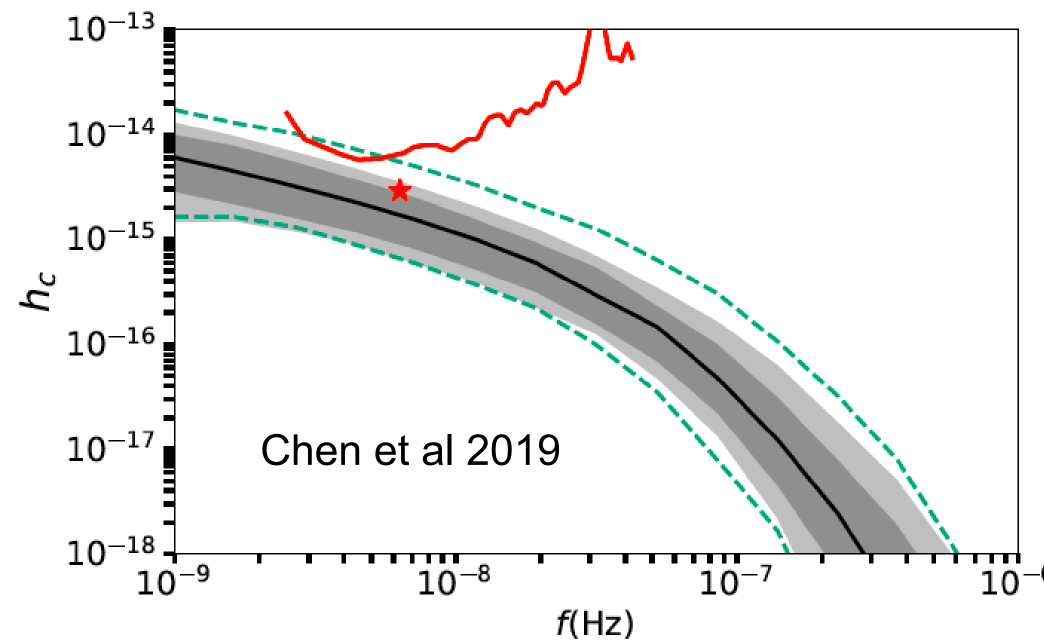

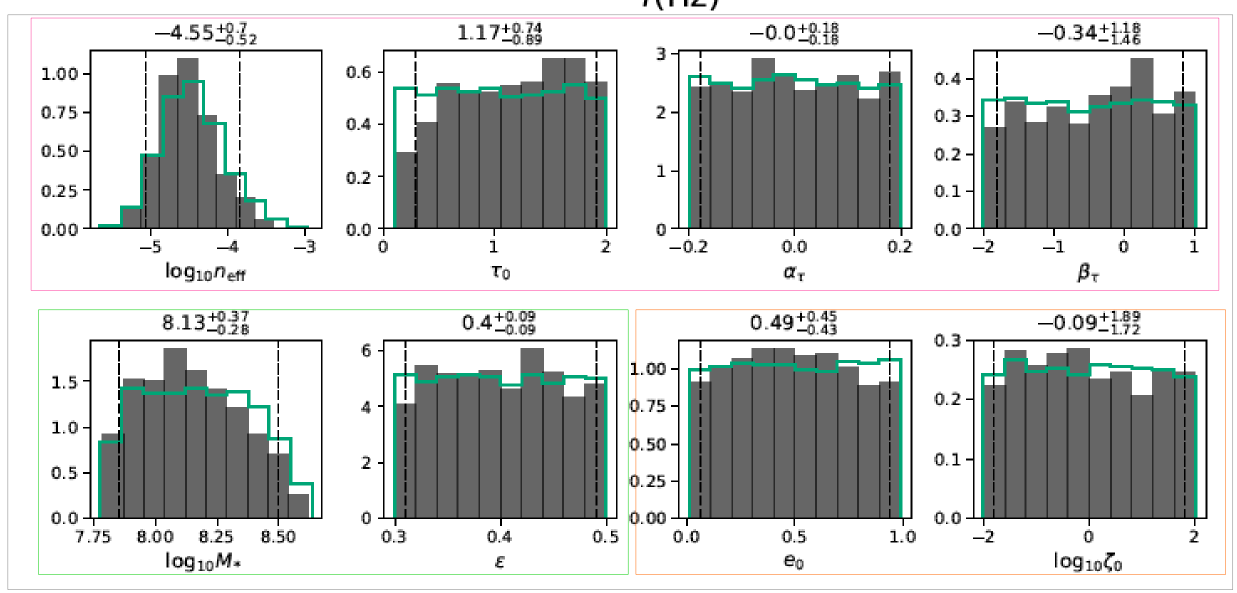

Constraints on astrophysical models

Chen et al 2019
EPTA – population synthesis

parameter	description	standard	extended
	Galaxy stellar mass function		
Φ_0	GSMF norm	-2.8 ± 0.3	-2.8 ± 0.3
Φ_I	GSMF norm redshift evolution	-0.25 ± 0.22	-0.25 ± 0.22
$\log_{10}M_0$	GSMF scaling mass	11.25 ± 0.2	11.25 ± 0.2
α_0	GSMF mass slope	-1.25 ± 0.17	-1.25 ± 0.17
α_I	GSMF mass slope redshift evolution	0 ± 0.15	0 ± 0.15
	Pair fraction		
f_0	pair fraction norm	[0.02,0.03]	[0.01,0.05]
α_f	pair fraction mass slope	[-0.2,0.2]	[-0.5,0.5]
β_f	pair fraction redshift slope	[0.6,1]	[0,2]
γ_f	pair fraction mass ratio slope	[-0.2,0.2]	[-0.2,0.2]
	Merger timescale		
τ_0	merger time norm	[0.1,2]	[0.1,10]
α_τ	merger time mass slope	[-0.2,0.2]	[-0.5,0.5]
β_τ	merger time redshift slope	[-2,1]	[-3,1]
γ_τ	merger time mass ratio slope	[-0.2,0.2]	[-0.2,0.2]
	M_{bulge} - M_{BH} relation		
$\log_{10}M_*$	$M_{\rm bulge}-M_{\rm BH}$ relation norm	8.17 ± 0.33	8.17 ± 0.33
α_*	$M_{\rm bulge}-M_{\rm BH}$ relation slope	1 ± 0.1	1 ± 0.1
ϵ	$M_{\rm bulge}-M_{\rm BH}$ relation scatter	[0.3,0.5]	[0.2,0.5]
	Eccentricity and stellar density		
e_0	binary eccentricity	[0.01,0.99]	[0.01,0.99]
$\log_{10}\zeta_0$	stellar density factor	[-2,2]	[-2,2]

Case of no-detection

Strain limit : $A(f=\mathrm{yr}^{-1}) = 1\times10^{-16}$

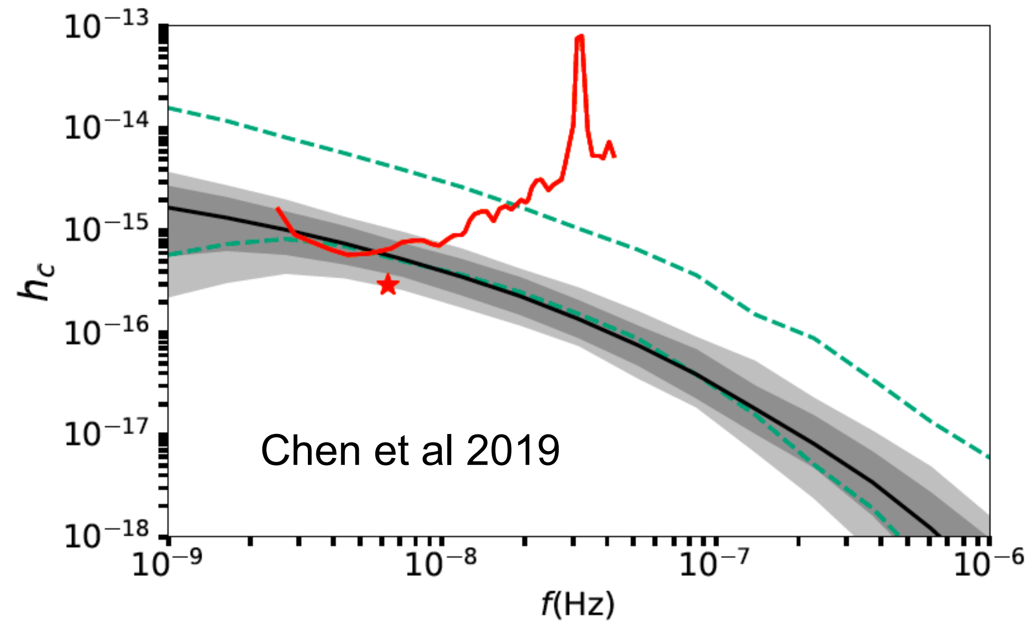

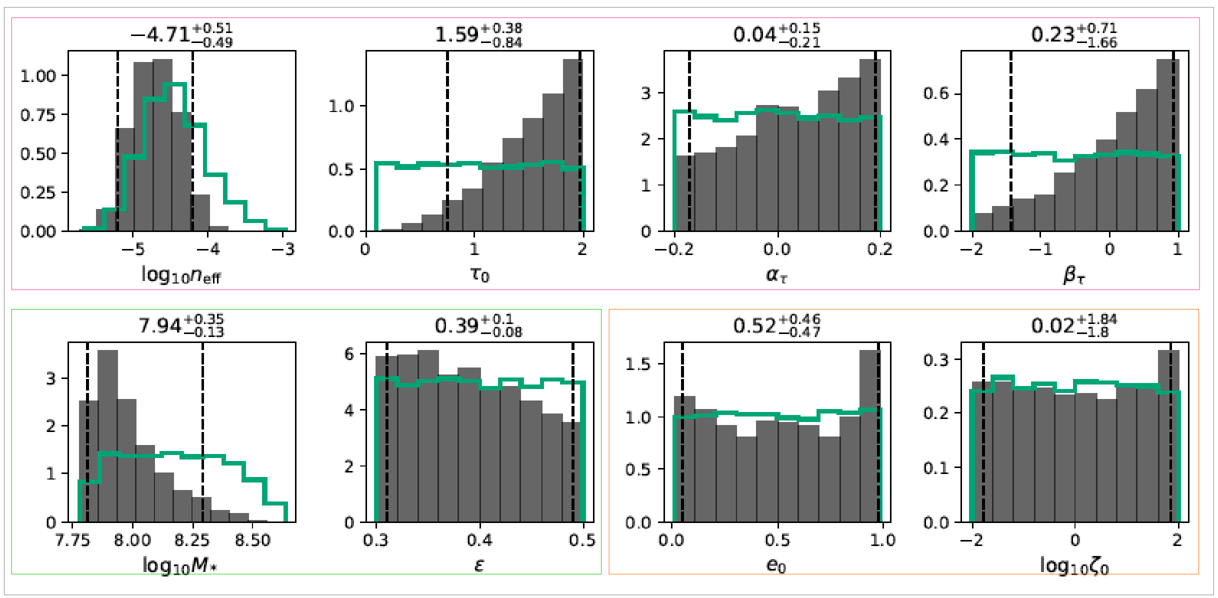

Constraints on astrophysical models

Chen et al 2019
EPTA – population synthesis

parameter	description	standard	extended
Φ_0	GSMF norm	-2.8 ± 0.3	-2.8 ± 0.3
Φ_I	GSMF norm redshift evolution	-0.25 ± 0.22	-0.25 ± 0.22
$\log_{10} M_0$	GSMF scaling mass	11.25 ± 0.2	11.25 ± 0.2
α_0	GSMF mass slope	-1.25 ± 0.17	-1.25 ± 0.17
α_I	GSMF mass slope redshift evolution	0 ± 0.15	0 ± 0.15
f_0	pair fraction norm	[0.02,0.03]	[0.01,0.05]
α_f	pair fraction mass slope	[-0.2,0.2]	[-0.5,0.5]
β_f	pair fraction redshift slope	[0.6,1]	[0,2]
γ_f	pair fraction mass ratio slope	[-0.2,0.2]	[-0.2,0.2]
τ_0	merger time norm	[0.1,2]	[0.1,10]
α_τ	merger time mass slope	[-0.2,0.2]	[-0.5,0.5]
β_τ	merger time redshift slope	[-2,1]	[-3,1]
γ_τ	merger time mass ratio slope	[-0.2,0.2]	[-0.2,0.2]
$\log_{10} M_*$	$M_{\rm bulge} - M_{\rm BH}$ relation norm	8.17 ± 0.33	8.17 ± 0.33
α_*	$M_{\rm bulge} - M_{\rm BH}$ relation slope	1 ± 0.1	1 ± 0.1
ϵ	$M_{\rm bulge} - M_{\rm BH}$ relation scatter	[0.3,0.5]	[0.2,0.5]
e_0	binary eccentricity	[0.01,0.99]	[0.01,0.99]
$\log_{10} \zeta_0$	stellar density factor	[-2,2]	[-2,2]

Galaxy stellar mass function

Pair fraction

Merger timescale

M_{bulge} -M_{BH} relation

Eccentricity and stellar density

Middleton et al 2021

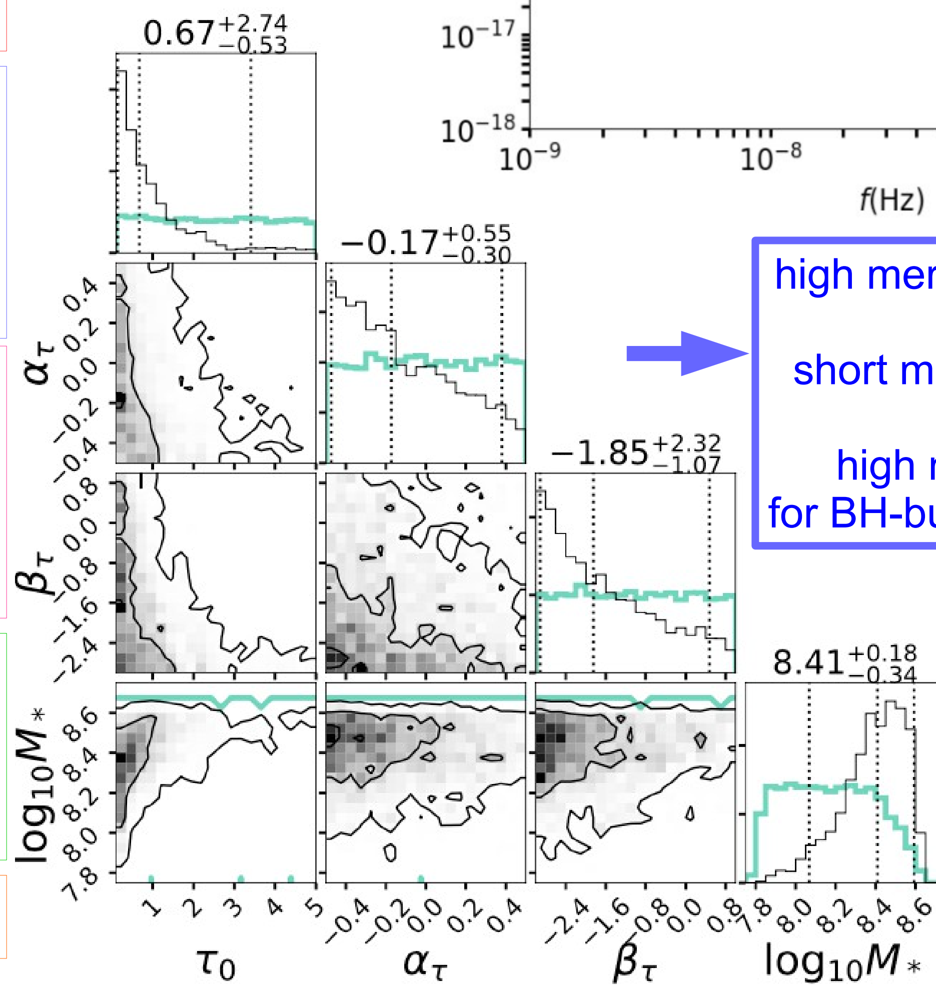

case of a common red signal with $h_c \sim 2.\ 10^{-15}$?

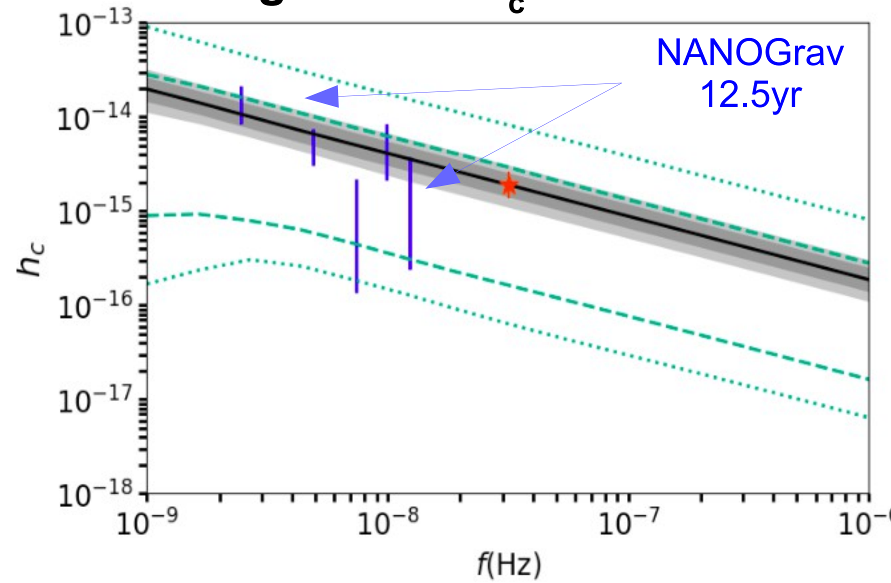

high merger rate densities

short merger timescales

high normalization for BH-bulge mass relation

An essential diagnostic : the spatial correlation of the signal

The gravitational signal is contained in the covariance matrix C of the arrival time residuals r(t)

It is decomposed into a sum of « noises » whose spectrum is described by a power law

$$S \propto A^2 f^{-\gamma}$$

$$C \sim \Gamma_{ab}\rho_i\delta_{ij} + \epsilon_i\delta_{ij} + \eta_i\delta_{ab}\delta_{ij} + \kappa_{ai}\delta_{ab}\delta_{ij}$$

GW clock/eph. astroφ indiv. rot./disp.

the covariance matrix C depends both on the amplitude of the signal as a function of its sky position and on the «antenna pattern »

$$\Gamma_{ab} = \frac{3}{8\pi}(1+\delta_{ab})\int_{S^2} d\hat{\Omega}\; P(\hat{\Omega}) \sum_q F_a^q(\hat{\Omega})F_b^q(\hat{\Omega})$$

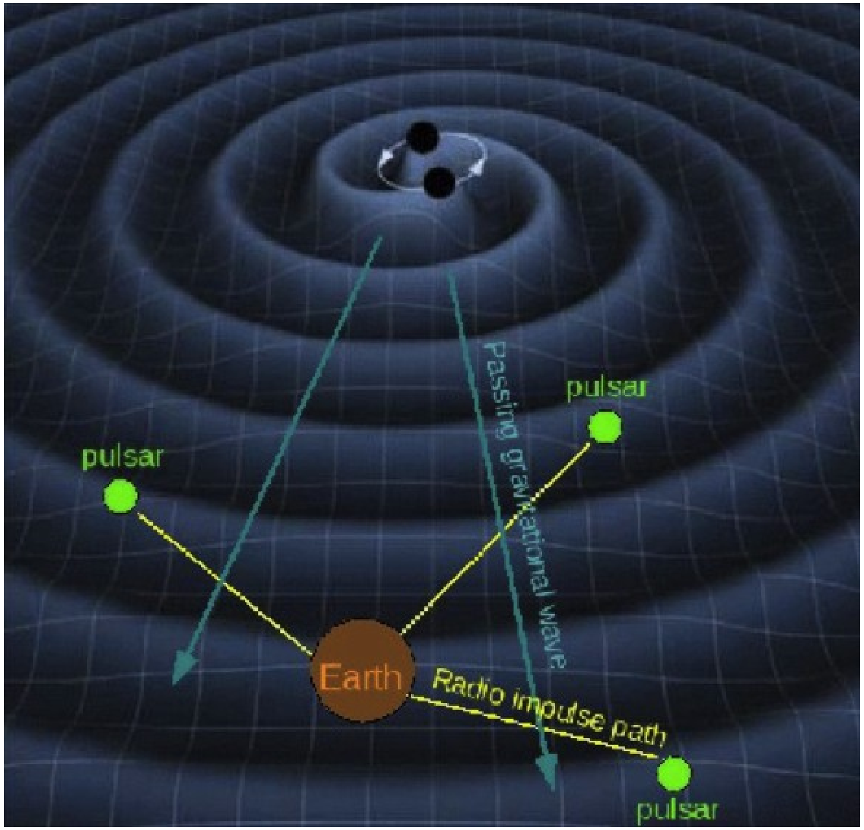

An essential diagnostic : the spatial correlation of the signal

The gravitational signal is contained in the covariance matrix C of the arrival time residuals r(t)

It is decomposed into a sum of « noises » whose spectrum is described by a power law

$$S \propto A^2 f^{-\gamma}$$

$$C \sim \underbrace{\Gamma_{ab}\rho_i\delta_{ij}}_{\text{GW}} + \underbrace{\epsilon_i\delta_{ij}}_{\text{clock/eph.}} + \underbrace{\eta_i\delta_{ab}\delta_{ij}}_{\text{astro}\varphi} + \underbrace{\kappa_{ai}\delta_{ab}\delta_{ij}}_{\text{indiv. rot./disp.}}$$

GW clock/eph. astroφ indiv. rot./disp.

the covariance matrix C depends both on the amplitude of the signal as a function of its sky position and on the «antenna pattern »

$$\Gamma_{ab} = \frac{3}{8\pi}(1+\delta_{ab})\int_{S^2} d\hat{\Omega}\, P(\hat{\Omega}) \sum_q F_a^q(\hat{\Omega})F_b^q(\hat{\Omega})$$

Earth term: the stochastic signal is spatially correlated between all pulsars as a function of their angular separation

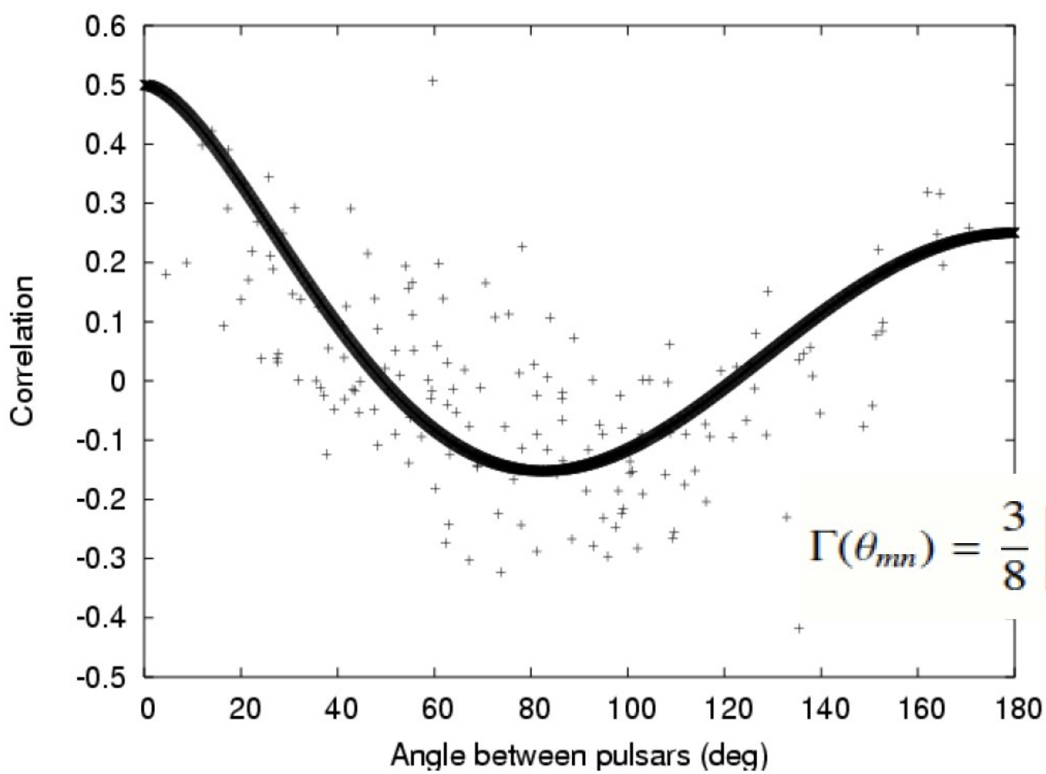

Cf Hellings & Downs 1983

solution for an isototropic background :

$$\Gamma(\theta_{mn}) = \frac{3}{8}\left[1 + \frac{\cos\theta_{mn}}{3} + 4(1-\cos\theta_{mn})\ln\left(\sin\frac{\theta_{mn}}{2}\right)\right](1+\delta_{mn})$$

An essential diagnostic : the spatial correlation of the signal

Not detected yet !

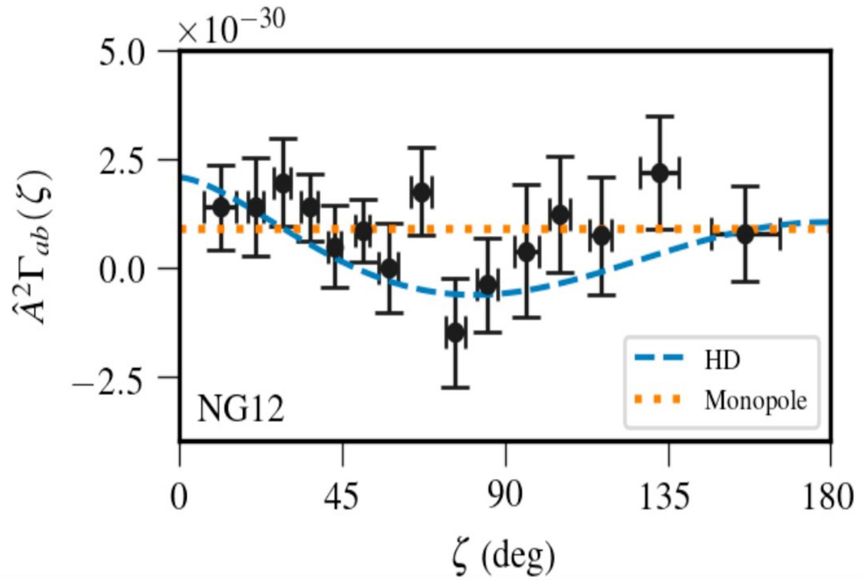

47 pulsars

NANOGrav ; Arzoumanian et al 2020

17 pulsars

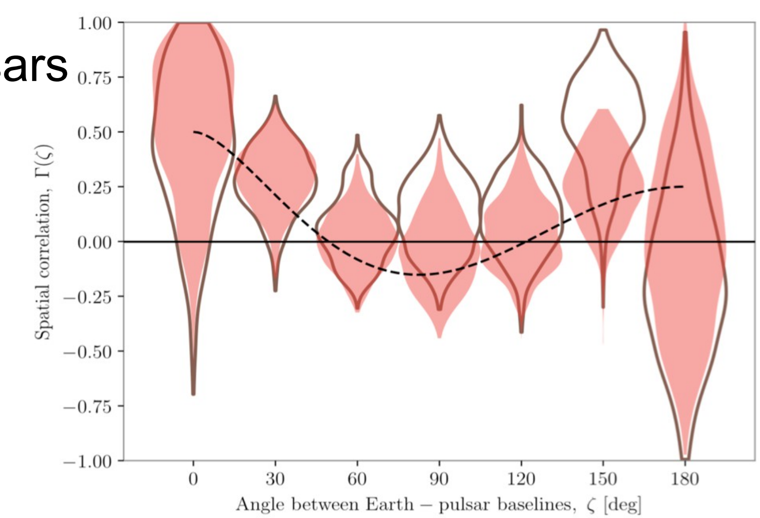

PPTA ; Goncharov et al 2021

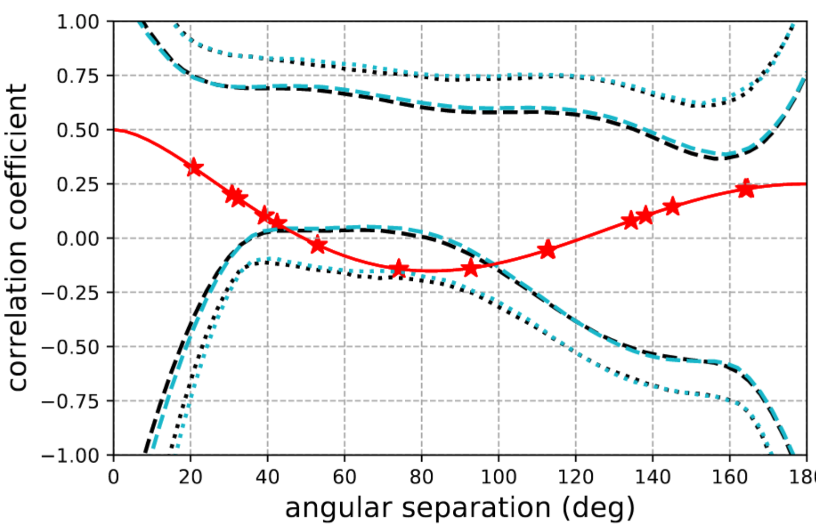

6 pulsars

EPTA – 6 best ; Chen et al 2021

We cannot distinguish yet a common uncorrelated red noise of some astrophysical origin from a GW stochastic background

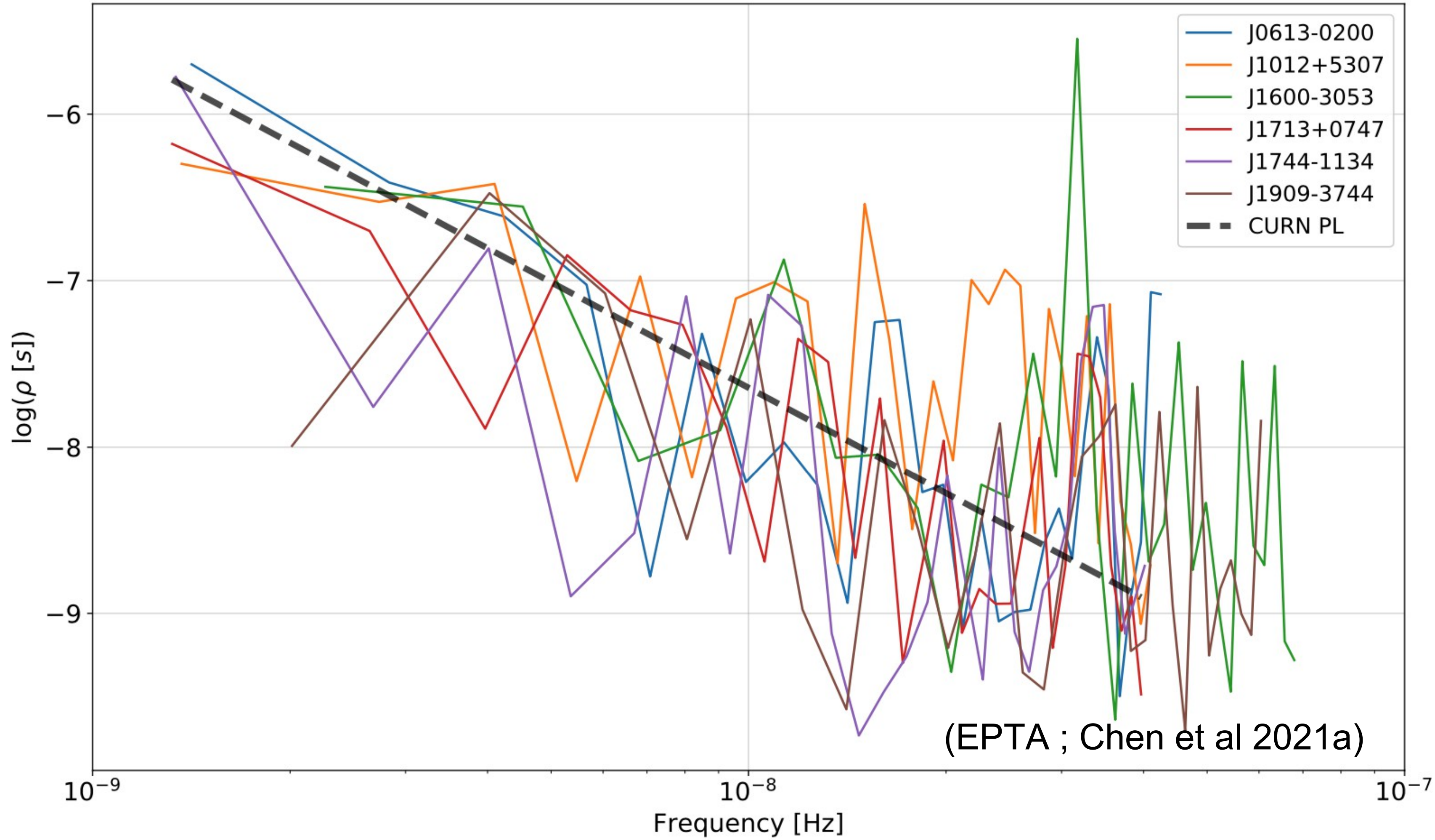

Compaparing **individual pulsar noise** models to inferred **Common Uncorrelated Red Noise**

Follow-up results

1) confirmation using IPTA-DR2
= combination of « old » data
(EPTA 15 years, NANOGrav 9 years, PPTA 6 years)

Antoniadis et al 2022

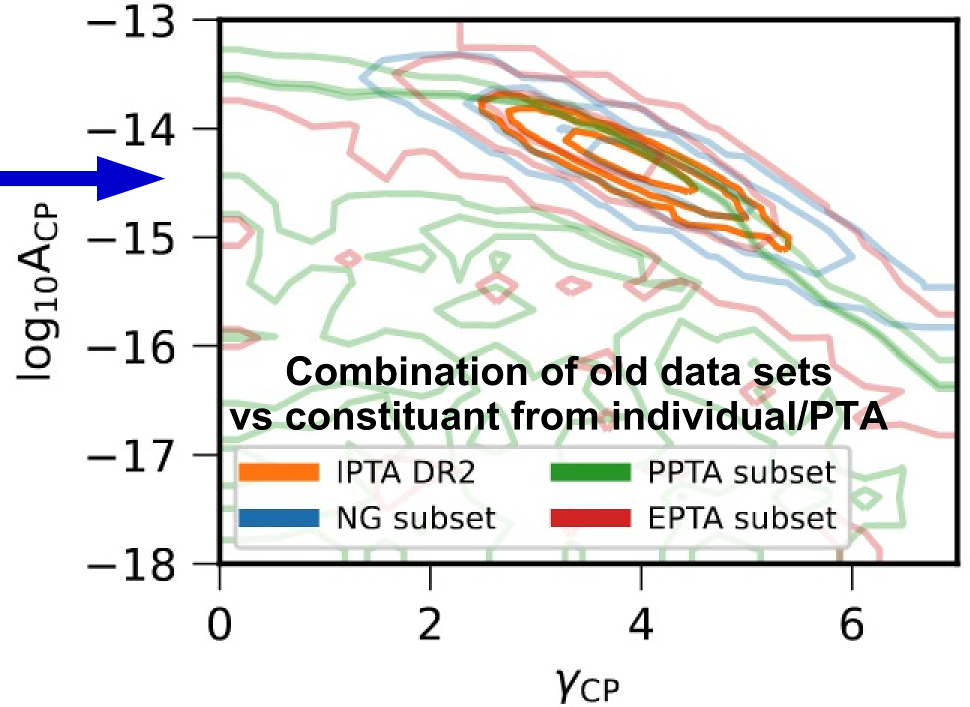

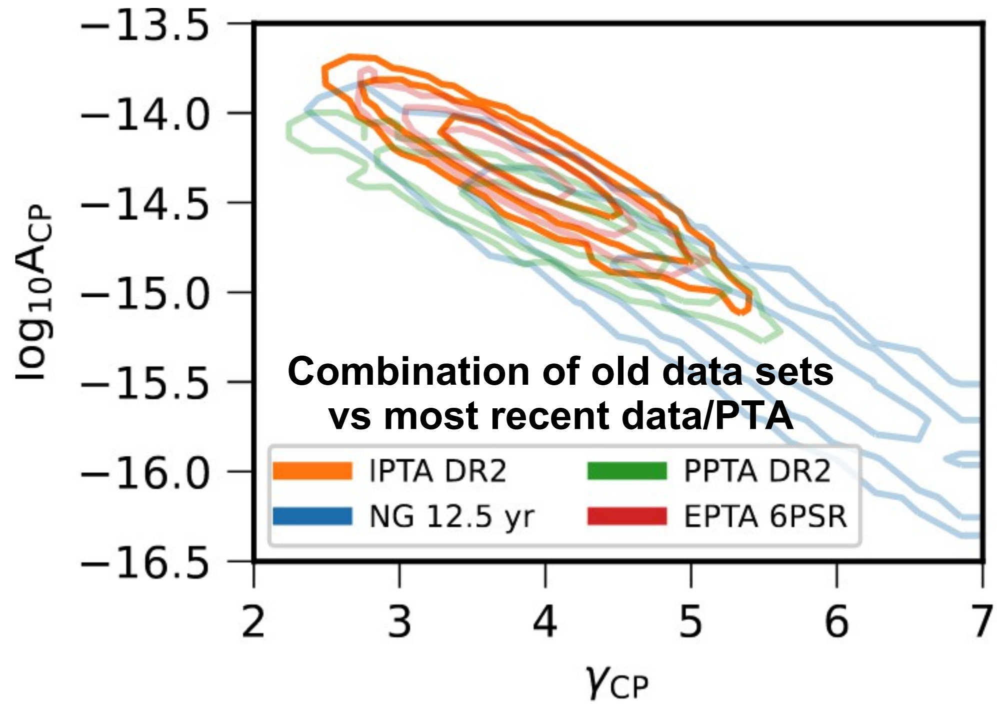

Follow-up results

1) confirmation using IPTA-DR2
= combination of « old » data
(EPTA 15 years, NANOGrav 9 years, PPTA 6 years)

Antoniadis et al 2022

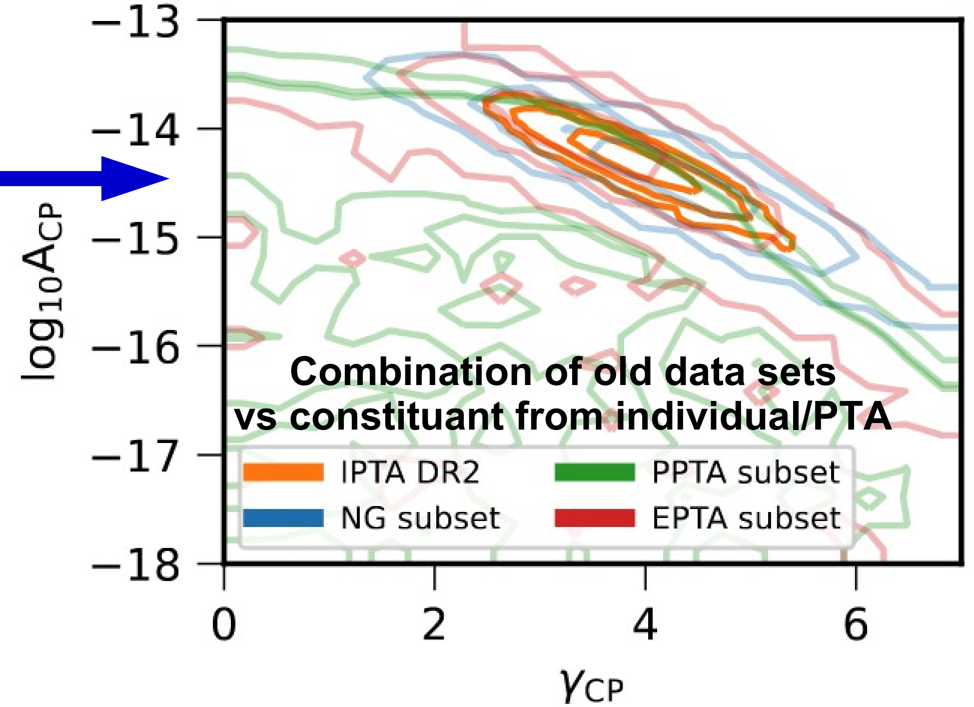

2) <u>« 3+ paper agreement » (late 2022)</u>

→ building extended data sets
→ issue = clear detection of the spatial correlation of the signa
l
→ a common detection check list

EPTA (+InPTA)	6 → 26 pulsars,	T = 25 years
PPTA	17 → 26 pulsars,	T = 25 years
NANOGrav	47 → 60 pulsars,	T = 15 years

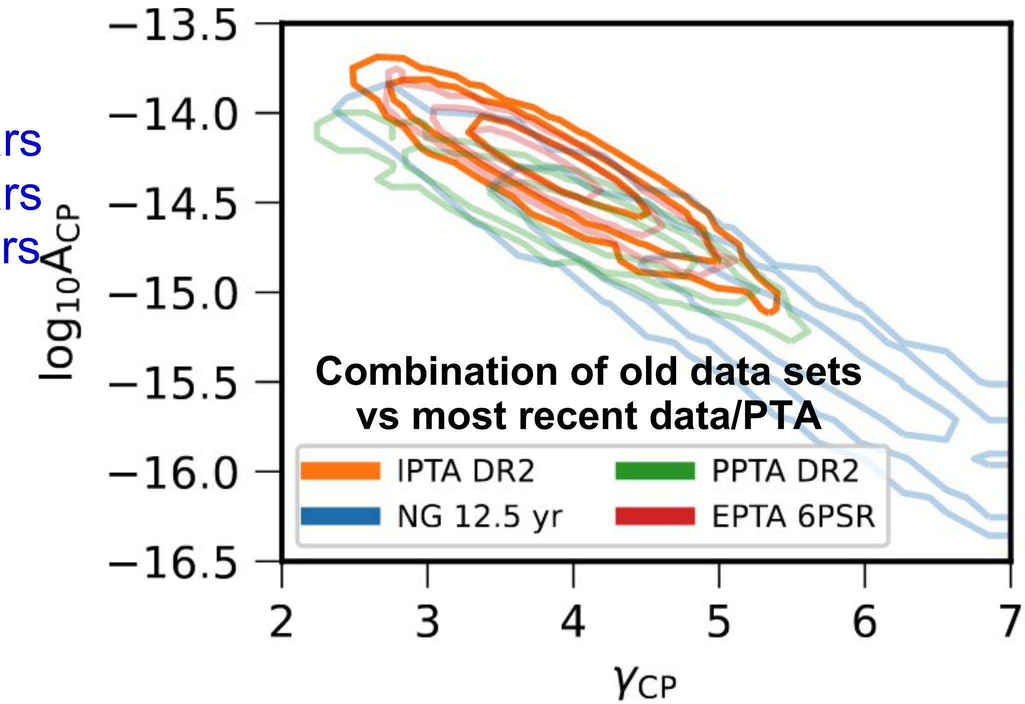

3) IPTA DR3 release (late 2023?)
= combination of the three new data sets
+ 3 years MeerKAT + 3 years FAST

Follow-up results

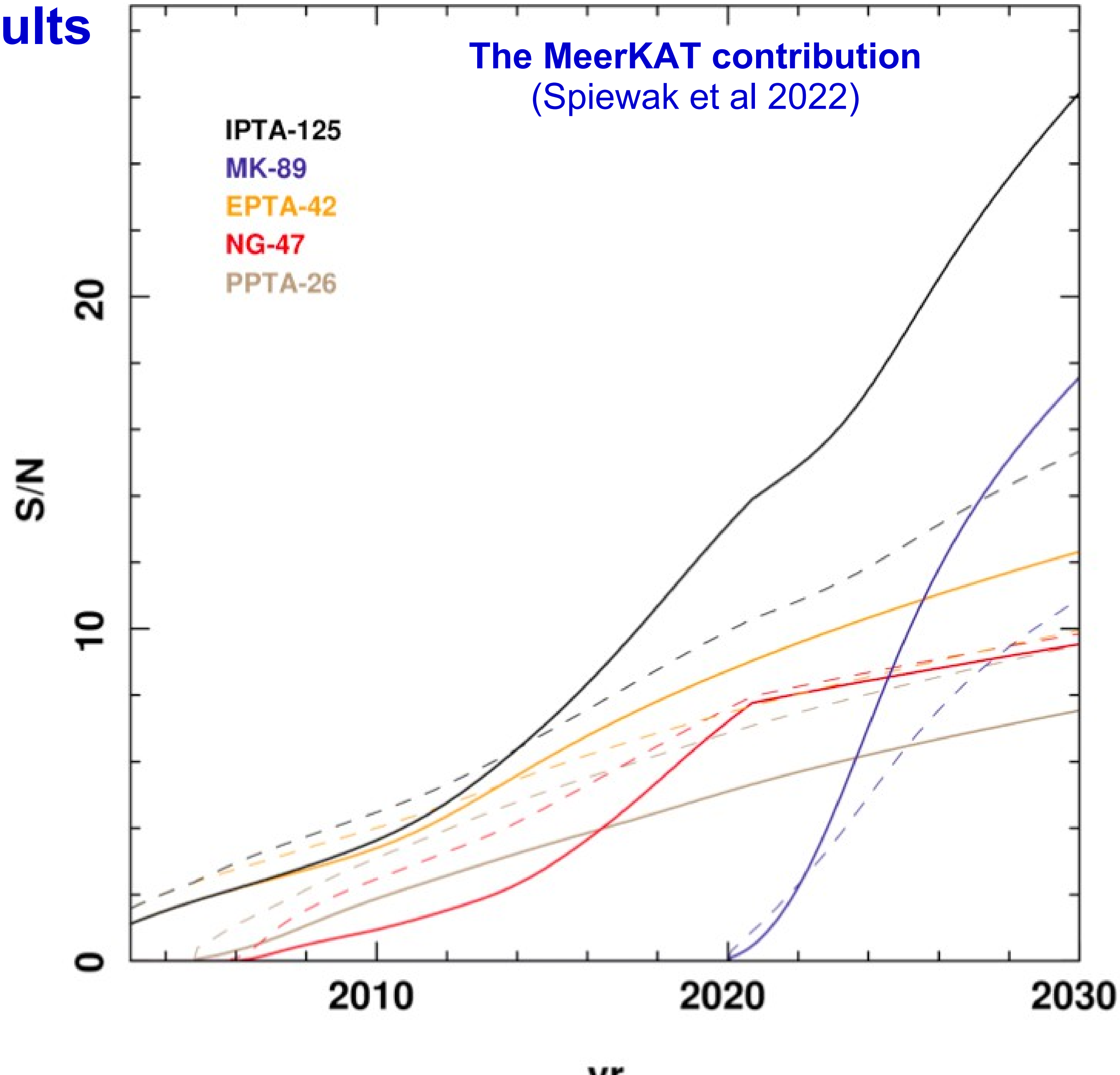

Work in progress...

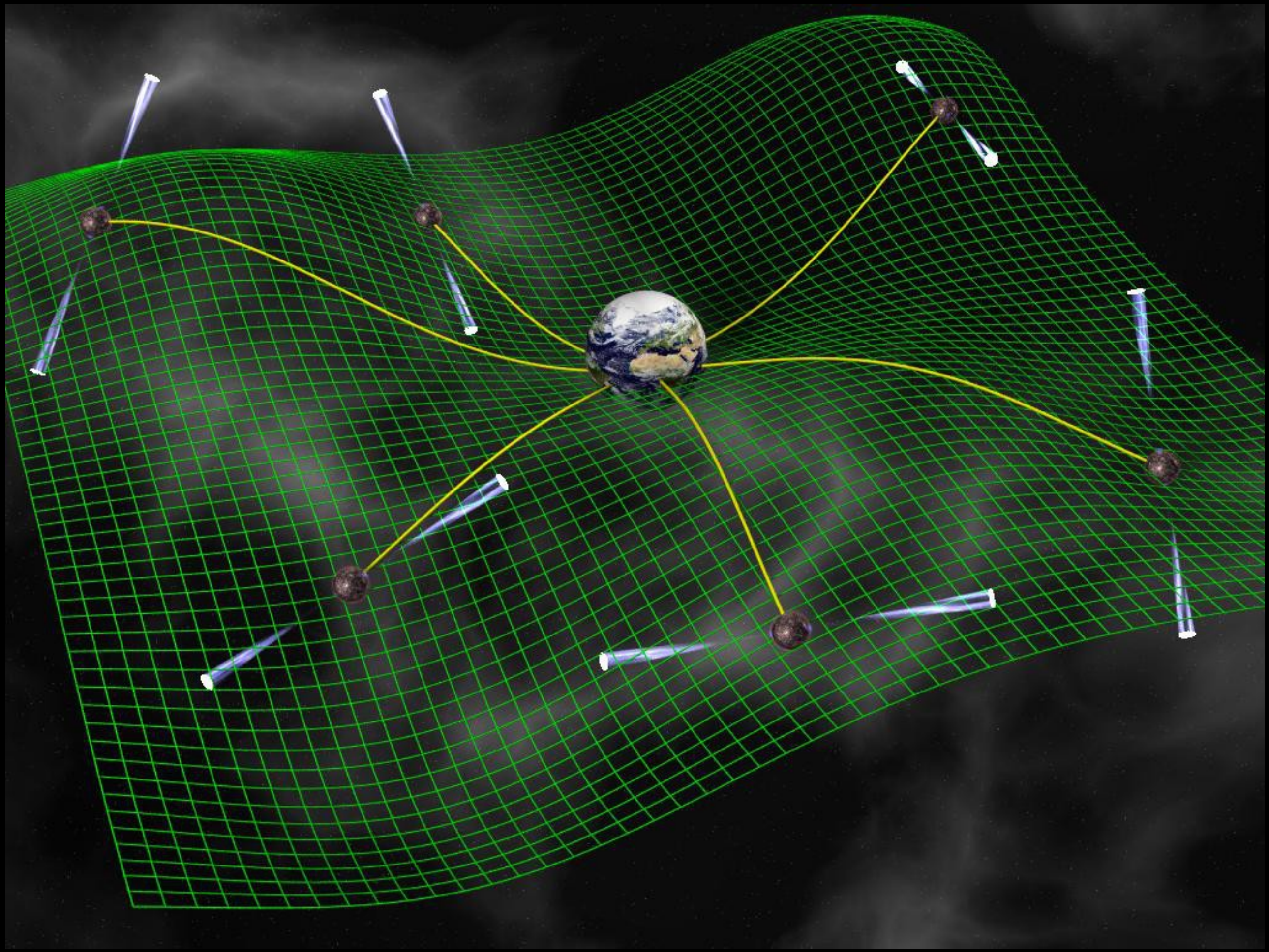

Expect interesting results in the coming year